Validation of Oil Spill Transport and Fate Modeling in Arctic Ice

Authors:

*[1]Deborah P. French-McCay, [1]Tayebeh Tajalli-Bakhsh, [1]Kathy Jayko, [2]Malcolm L. Spaulding, and [3]Zhengkai Li

[1]RPS ASA

55 Village Square Drive

South Kingstown, RI 02879 USA

Debbie.FrenchMcCay@rpsgroup.com

Tayebeh.TajalliBakhsh@rpsgroup.com

Kathy.Jayko@rpsgroup.com

[2] Department of Ocean Engineering, University of Rhode Island

South Ferry Road, Narragansett, RI 02882 USA

spaulding@oce.uri.edu

[3] PureLine Treatment Systems

1241 N. Ellis Street

Bensenville, IL 60106 USA

zkli06@gmail.com

Running Header: Oil Spill Modeling in Ice

ABSTRACT

Reliability of oil spill modeling in Arctic waters for response planning and risk assessments depends on the accuracy of winds, currents, and ice data (cover and drift) used as input. We compared predicted transport in ice, using ice and ocean model results as input, with observed drifter trajectories in the Beaufort Sea and an experimental oil release in the Barents Sea. The ice models varied in ice rheology algorithms used (i.e., Elastic-Viscous-Plastic [EVP], presently used in climate models, versus a new Elasto-Brittle [EB] approach in pack ice) and the time averaging of their outputs, which were provided as input to oil spill models. Evaluations of model performance (skill) against drifters showed improvement using EB instead of EVP rheology. However, model skill was degraded by time-averaging of ocean and ice model vectors before input to the oil spill model. While the accuracy of individual oil model trajectories projected weeks to months into the future is expected to be low, in the event of a spill, forecasts could be updated frequently with satellite and other observations to improve reliability. Comparisons of modeled trajectories with drifters verified that use of the ice-ocean models for ensemble modeling as part of risk assessments is reliable.

Key words: trajectory model, ice drifter, ice model, Arctic spill response, oil weathering in ice

INTRODUCTION

For simulation of oil spill trajectory and fate in Arctic waters, oil spill models depend upon ice, ocean (hydrodynamic) and meteorological models to provide wind, current, and ice drift rates, coverage, and thickness. For contingency planning and risk assessment studies, sufficiently reliable sea ice data are needed to predict potential oil exposure useful for making decisions regarding permitting and spill response strategies. At the planning stage for a new drilling application, models are used to predict an ensemble suite of possible spill trajectories over periods of weeks to months using hindcast wind and current data. The results of these trajectories are used to assign probabilities of certain ocean or shoreline areas becoming oiled based on historical metocean data. This information in turn provides graphic pictures of spatial risk for developing response plans, staging resources and conducting the overall environmental assessment (EA) for the project.

Once drilling begins, oil spill models form a stand-by support tool ready to assist responders in an emergency by predicting where the oil is going and at what rate. In this real-time response application, oil spill models are run to generate forecasts of generally 3 – 5 days duration recognizing that beyond this time scale, the wind forecast accuracy degrades quickly. However, available ice and ocean model systems were designed primarily for evaluating Arctic-scale climate-related issues. They have been of lower spatial/temporal resolution and accuracy than desirable for operational oil spill model forecasts in ice-infested waters.

This oil-in-ice trajectory modeling study evaluated the increase in model accuracy achievable by using recent developments in ice modeling / forecasting capabilities. The improved ice and ocean models were integrated with existing oil spill transport and fate models and model forecast performance was evaluated.

RESEARCH INITIATIVES

Arctic Oil Spill Response Technology – JIP Programme

The International Association of Oil and Gas Producers (IOGP), in support of the Arctic Oil Spill Response Technology – Joint Industry Programme (JIP), sought to advance and expand the oil and gas industries' oil spill modeling capabilities within the Arctic via enhancement of established industry oil trajectory and fate models used for support of IOGP members' interests. The JIP recognized that available ice model products, designed primarily for evaluating Arctic-scale and climate-related issues, were of lower resolution and accuracy than desirable for required high resolution oil spill forecast modeling in ice-infested waters. Thus, Phase 1 of the initiative focused on improving ice modeling algorithms and the resolution of ice dynamics and Phase 2 was to make use of the updated ice modeling products in oil spill models to evaluate performance.

Ice and Ocean Models

There are a number of sea ice models for the Arctic Ocean that are forced by operational global ocean (hydrodynamic) models. The EUROGOOS (European Global Ocean Observing System) website [http://eurogoos.eu/models/] provides a catalogue of, and links to, existing global, regional and coastal ocean models generated from the GOOS Regional Alliances (GRAs). The Arctic Ocean models include those built off the Nucleus for European Modelling for the Ocean (NEMO) system (used by the Finnish Meteorological Institute, U.K. Met Office, and Mercator Ocean), which is coupled with the thermodynamic-dynamic sea ice model Louvain-la-Neuve Sea Ice Model (LIM; http://www.elic.ucl.ac.be/repomodx/lim/); the Helsinki Multi-category sea-Ice model (HELMI) developed by the Finnish Meteorological Institute (Haapala et al. 2005, Mårtensson et al. 2012); and the (Towards) an Operational Prediction system for the North Atlantic European coastal Zones (TOPAZ; http://topaz.nersc.no/) developed by Nansen Environmental and Remote Sensing Centre (NERSC), Bergen, Norway, which was the focus of this study. TOPAZ4 is currently the Arctic Ocean forecast platform within the European monitoring and forecast service MyOcean (http://eurogoos.eu/modelling_inventory/eurogoos-136/). Forecast products are available at [http://eurogoos.eu/roos/arctic-roos/]. Predicted transport using TOPAZ and associated models developed by NERSC (Ólason et al. 2016) was evaluated to examine model performance.

TOPAZ4 incorporates the HYCOM hydrodynamic model version 2.2 (Bleck 2002), with 28 vertical layers divided into isopycnal layers in the stratified interior of the open ocean and z-coordinates in the unstratified surface mixed layer. The ocean model is coupled to a one thickness category sea ice model using an elastic-viscous-plastic (EVP) rheology (Hunke and Dukowicz 1997). A 100-member ensemble Kalman filter (EnKF; Evensen 1994) is used to assimilate remotely-sensed sea level anomalies, sea surface temperature, sea ice concentration, Lagrangian sea ice velocities (winter only), as well as temperature and salinity profiles from Argo floats. Wind stress for the TOPAZ4 model is from the ERA-40 (European Center for Medium-range Weather Forecast, ECMWF RE-ANALYSIS) wind model (https://www.ecmwf.int/en/research/climate-reanalysis). The applied atmospheric forcing fields are the 6-hourly 10-meter wind velocities from the ERA interim reanalysis (ERAi) distributed at

80 km spatial resolution (http://www.ecmwf.int/en/research/climate-reanalysis/era-interim). The performance of the model has been compared to data in broad scale; Sakov et al. (2012) found that TOPAZ4 produced realistic estimates of the mesoscale circulation in the North Atlantic and sea ice variability within the Arctic. The horizontal resolution of TOPAZ4 is approximately 12-16 km in the Arctic Ocean.

Recently NERSC (Ólason et al. 2016) updated their ice modeling approach and specifically the rheology for pack ice. The resulting Lagrangian-based Elasto-Brittle (EB) model named neXtSIM (Rampal et al. 2009a), which uses a more accurate rheology for pack ice than classic models (which use EVP), showed significant improvement in performance under heavy ice conditions over the present (Elastic-Viscous-Plastic, EVP) modeling approach used in their operational TOPAZ4 coupled ice-ocean model. The EB-based neXtSIM model better preserves dynamic features like cracks, ridges, and leads in pack ice than traditional Eulerian models (Rampal et al. 2016a). NERSC focused their validation (Rampal et al. 2016b) on examination of transport (as compared to drifters and interpretations of satellite imagery), statistical analysis of ice coverage, and on the degree of dispersion (comparing model predictions to drifters). In comparing model predictions to drifter paths in the Beaufort Sea, NERSC noted that the predicted westward ice movements were too fast using TOPAZ coupled with the standard EVP rheology, but more similar to observations using the neXtSIM model.

Phase 1 and 2 of JIP Programme

NERSC (Ólason et al. 2016) performed the JIP Phase 1 ice modeling efforts, focusing on three model developments: (1) a discrete element model (DE) for the Marginal Ice Zone (MIZ); (2) the EB ice rheology model, which is an advancement over the standard (historically-used)

EVP rheology algorithm for the ice pack; and (3) integration of a wave-in-ice model (WIM) into a high-resolution version of their TOPAZ ocean and ice model. NERSC identified the Discrete Element (DE) model as superior under MIZ conditions and the EB as best in heavy (pack) ice. NERSC ran the DE model for a limited area and time span as part of Phase 1, showing that "the DE model delivers unprecedented realism in terms of the simulation of ice floe interactions". However, they concluded that the DE model is computationally intensive, requiring considerable memory and time to run, and is not ready for operational use (Ólason et al. 2016). Output of the DE model was therefore not provided for use in the oil spill modeling. Ólason et al. (2016) also conclude: "The main drawback of the current version of the EB model is that it cannot yet be coupled to a full ocean or atmospheric model, resulting in limited feedbacks from these systems on the modelled ice."

For input to oil spill modeling, NERSC (Ólason et al. 2016) provided data products (Table 1) for defined areas of the Beaufort Sea and the Barents-Kara Seas (Figure S1 in Supplementary Material). The TOPAZ-EVP-WIM data were provided for small areas within each of the Beaufort Sea and the Barents and Kara Seas, and for five individual months. Note that the three TOPAZ models differed in the rheology and the hydrodynamics used. Also, the neXtSIM EB model used different winds than were used for the TOPAZ model runs. As the neXtSIM EB model was only run for winter months with large areas of pack ice, the three NERSC model products had common time periods within three individual months: March 2008, December 2008 and May 2009.

The focus of Phase 2 of the initiative and this work was to make use of the updated ice modeling products in RPS ASA's oil trajectory and fate models (OIL and Spill Impact

MAPping, OILMAP and SIMAP) and validate the simulated transport with *in situ* drifter data and observational data from an experimental oil release in the Barents Sea.

METHODS

Approach

The three refined ice modeling products provided by NERSC (Ólason et al. 2016) as part of Phase I of the JIP project, as well as publically-available TOPAZ4 data products, were used to evaluate potential improvements in modeling oil transport by comparison to observed movements by International Arctic Buoy Programme (IABP) drifters. Since IABP buoys were not available in the Kara-Barents Sea domain for the time window of interest, the study focused on comparison of modeled trajectories to observed drifter paths in the Beaufort Sea. The four ice-ocean model products used were:

1. TOPAZ-EVP: TOPAZ hydrodynamics and ice model using updated EVP rheology, free-run (i.e., with no data assimilation) for 10-years (2001-2010), provided as 6-hourly averages.
2. TOPAZ-EVP-WIM: High resolution (i.e., temporally; grid is same as TOPAZ_EVP) TOPAZ (free-run) hydrodynamics and ice model using updated EVP and MIZ rheology, as well as WIM-generated wave data in the MIZ, for hindcasts of 5 selected months (March, June, September, and December of 2008 and May 2009) in a portion of the Beaufort Sea, provided as hourly data.

3. neXtSIM: Updated TOPAZ reanalysis hydrodynamics and ice model with EB rheology in pack ice, run for 10 winter periods (i.e., November 1 – May 15, 2000-2010), provided as 6-hourly averages.
4. TOPAZ4: publically available product from the operational model; hydrodynamics and ice models in reanalysis mode, with ice model using the standard EVP rheology.

Using trajectory simulations, we have compared transport using NERSC ice-ocean model datasets against available *in situ* drifter data in the ice model product domains of the Beaufort Sea from the IABP. In addition to examining the oil transport predictions, we have evaluated the potential improvements and implications of the changes resulting from use of the updated ice-ocean model products on oil spill trajectory and fate modeling that is used for exposure analyses of resources at risk in the Arctic.

Oil Spill Model Algorithms

The model algorithms in OILMAP and SIMAP (French-McCay 2003, 2004; French-McCay et al. 2017) have been developed over the past three decades to simulate oil transport and fate under a variety of environmental conditions. The SIMAP model quantifies trajectory, areas swept by floating oil of varying thicknesses, and fates and concentrations of subsurface oil components (dissolved and particulate). Processes simulated include spreading (gravitational and by shear), evaporation of volatiles from surface oil, transport on the surface (in ice and open water) and in the water column, randomized dispersion from small-scale motions (turbulent mixing), emulsification, entrainment and resurfacing of oil as droplets of varying sizes into the water (natural and facilitated by dispersant application) or returned to the surface, dissolution of soluble components, volatilization of dissolved hydrocarbons from the surface water, adherence of oil droplets to suspended sediments, adsorption of soluble and semi-soluble aromatics to suspended sediments, sedimentation, stranding on shorelines and landfast ice edges, and degradation. Lower-molecular-weight aromatic hydrocarbons, i.e., mono-aromatics (MAHs) and polynuclear aromatic hydrocarbons (PAHs), are the soluble and semi-soluble components that are most bioavailable to aquatic biota, inducing most of the effects (French-McCay 2002). These and other "pseudo-components" representing volatile aliphatic hydrocarbons are tracked separately from residual oil in the model. Whole oil (containing non-volatile residual oil and volatile components not yet volatilized or dissolved from the oil) is simulated as floating slicks, emulsions and/or tarballs, oil in ice, or as dispersed oil droplets of varying diameter (some of which may resurface). Sublots of the spilled oil are represented by Lagrangian elements ("spillets"), each characterized by mass of hydrocarbon components and water, location, thickness, diameter, density, and viscosity. A separate set of Lagrangian elements is used to track movement of the dissolved hydrocarbons.

OILMAP is a simplified version of SIMAP, as it is designed for operational use and for contingency planning. OILMAP uses a reduced number of pseudo-components to represent the oil, and so requires less data than SIMAP to define the oil composition. OILMAP tracks the whole oil and volatiles through evaporation, but does not track dissolution or the transport and fate of the dissolved hydrocarbons.

Figure S2 (Supplementary Material) shows the model system and linkages to forcing (input) data from meteorological, ice, ocean, and wave models, as well as to a near field blowout model, OILMAP Deep, used to develop initial conditions from subsurface oil and gas releases. For pipeline and vessel spills, the release rates are parameterized in terms of the time history of the release. Response actions (e.g., dispersant application, booming, mechanical recovery, and *in situ* burning) can be implemented in the blowout and oil fate models, to account for changes in oil properties (i.e., from dispersant application), transport and fate due to these activities.

Oil interactions with mobile sea ice or immobile landfast ice involve several processes that affect oil transport and fate (see reviews by Drozdowski et al. 2011; Lee et al. 2011). Oil released at or above the water surface, may spill into water and/or onto the surface of the ice. Oil deposited on ice may absorb into surface snow, run off and become trapped between cracks or in open water between ice floes, and/or become encapsulated in the ice. On the other hand, oil released into and under water may become trapped under the ice in ridges and keels, or build up along and become trapped in sea or landfast ice edges (Drozdowski et al. 2011; Lee et al. 2011). Fate processes such as spreading, evaporation, dispersion, and emulsification are affected by the degree and characteristics of ice cover (e.g., see review by Afenyo et al. 2016). Many of these interactions and processes are at a finer scale than can be captured in oil spill models using inputs that are currently available from large scale meteorological, hydrodynamic and coupled ice-ocean models. However, the influence of ice on net transport and fate processes is simulated by considering the location of the oil (on, under or between ice) and potential reduction in oil surface area (i.e., reduced spreading), which changes the wave environment, entrainment rate, oil movement, dissolution, volatilization and mixing in the water column.

When oil interacts with mobile sea ice, some fraction will become contained (either on top, in, or underneath the ice) and will travel with the ice floes (Drozdowski et al. 2011). This oil can drift over great distances in the Arctic (Peterson et al. 2008). The fraction of oil moving with the ice versus that in open water depends on conditions and specifics of the release, ice coverage, subsurface ice roughness, winds and currents, and ice formation/melting dynamics (see detailed discussions in Drozdowski et al. 2011; Lee et al. 2011).

Transport Algorithms

Ice coverage information available in ice models is typically resolved at relatively large scales (>1 km). While detailed information regarding ice coverage and conditions are not available from these models, the information provided can be used as an indicator of whether oil would move predominantly with the surface water currents or with the ice. A rule of thumb followed by past modeling studies is that oil will generally drift with ice when ice coverage is greater than 30% (Drozdowski et al. 2011; Venkatesh et al. 1990). A recent review by experts on oil transport in ice-covered waters (CRRC 2016) concluded that up to 30% ice coverage, oil moves as though it is in open water, and at 80% and higher ice coverage oil transport is almost totally controlled by the ice. There is not agreement on how oil moves with intermediate ice coverage between 30% and 80%, i.e., in the MIZ. There is no specific field calibration for this guidance, although theoretical arguments have been made (Venkatesh et al. 1990; Lee et al. 2011; CRRC 2016). For example, as concluded in CRRC (2016): “The presence of frazil or brash ice between larger floes would increase control of the oil as compared to open water."

The OILMAP and SIMAP models use the ice coverage data (at the available resolution) to determine whether floating (or ice-trapped) oil is transported by the surface water currents or with the ice. In areas and at times where ice coverage is less than a minimum threshold defining the MIZ (MIZ_{min}, default assumption is 30%), floating oil is transported with surface water currents and a wind drift algorithm to account for wind-induced surface drift not resolved by the hydrodynamic model plus Stokes drift caused by wave motions. Wind drift is predicted in the oil spill model based on the modeling analysis of Stokes drift and Ekman flow by Youssef (1993) and Youssef and Spaulding (1993, 1994). According to this algorithm, in the northern hemisphere at moderate wind speeds, floating oil drifts 20^o to the right of downwind at about 3.5% of wind speed.

In areas and times where ice coverage exceeds MIZ_{min}, the ice coverage limits the spatial coverage of floating oil (not trapped under, in, or on ice) to the water between the ice, and the oil is transported with the ice using the ice velocities from the ice model. Within ice, the oil spill model utilizes and relies upon the ice model's calculation of transport of floating materials (by surface currents from the forcing hydrodynamic model and wind drift), which is represented by the ice movements. The ice model is assumed to capture changes in drift rate and angle under conditions from 100% ice to 30% ice cover. Oil trapped under, in or on ice moves with the ice, and oil between ice floes is assumed to move the same as the ice. Ice drift is typically about 2-4% of wind speed and in the Arctic it moves in a direction to the right of downwind (e.g., Faksness et al. 2010, observed drift rates equivalent to 3% of wind speed), similar to oil in open water (ASCE 1996).

A random walk dispersion process adds horizontal velocity to account for the advective dispersive processes below the scale of resolution of the input current and ice data. The dispersion velocities, u_{dd} and v_{dd} (m/s) in the east and north directions, respectively, are defined (Bear and Verruijt 1987) as

$$u_{dd} = \gamma\sqrt{\frac{2D_x}{\Delta t}}$$

$$v_{dd} = \gamma\sqrt{\frac{2D_y}{\Delta t}}$$

where D_x is horizontal dispersion coefficient in east-west direction (m^2/s), D_y is the horizontal dispersion coefficient in north-south direction (m^2/s), Δt is the time step, and γ is a random number (-1 to +1). D_x and D_y are assumed equal. The horizontal diffusion coefficients for floating oil characteristic of open water ($D_x = D_y = D_{xy}$) are reduced to $D_{xy'}$ in the ice, proportionately to percentage of ice cover (I_c) between MIZ_{min} and 100% ice cover.

$$D_{xy'} = D_{xy} \left(1 - (I_c - MIZ_{min})/(100 - MIZ_{min}) \right)$$

Immobile landfast ice that seasonally extends out from the coast may act as a natural barrier where oil can collect (Lee et al. 2011). In the model, when oil (moving in water with ice cover < MIZ_{min}) encounters landfast ice it is assumed to trap at or move along the ice edge (depending on the current and wind directions at the location and time). If oil becomes entrapped within landfast ice (by surfacing there or as landfast ice extends over the area), it remains immobile until the ice retreats. When landfast ice is no longer present at the location of trapped oil, the oil is released back into the water as floating oil.

<u>Oil Fate Processes</u>

In the presence of sea ice, weathering processes (e.g., evaporation and emulsification) and physical processes such as spreading and entrainment are slowed (Spaulding 1988). Wave-damping, the limitations on spreading dictated by the presence of sea ice, and temperature appear to be the primary factors governing observed spreading and weathering rates (Sorstrom et al. 2010).

As with transport, the ice coverage or concentration variable provided in the ice model is used as an index to control oil weathering and behavior processes in OILMAP and SIMAP (Table 2 summarizes the model algorithms). Oil behaves as it would in open water in ≤ MIZ_{min} ice coverage. Ice coverage exceeding the maximum percentage defining the MIZ (MIZ_{max}, default assumption is 80%, an adjustable model input) is assumed to be pack ice and effectively continuous ice cover. In the model, oil spilled on top of pack ice is allowed to evaporate, but does not spread from the initial condition of the release. (Note that feedback processes where oil cover increases ice melting in spring are not included, as the oil spill model is not coupled to the ice model.) Oil collected against the bottom surface or within ice does not spread (i.e., it is assumed to pool), evaporate/volatilize, emulsify or entrain into the water by surface waves. Oil dispersed below the ice moves with the local currents.

Oil spreading in ice coverage ≤ MIZ_{min} is the same as in open water. The spreading rate is reduced linearly based on ice cover, from no reduction from the open-water rate at MIZ_{min} to no spreading at MIZ_{max}. For ice cover > MIZ_{min}, spreading is constrained by the open water areal coverage within the ice. If the local temperature is below the oil's pour point, corrected for degree of weathering, it will not spread.

Laboratory and field studies have shown that oil weathering properties are strongly influenced by the low temperature, reduced oil spreading, and reduced wave action caused by moderate to high ice coverage (Brandvik et al. 2010a; Brandvik and Faksness 2009; Faksness et al. 2011). The weathering processes (e.g., evaporation and emulsification) in pack ice conditions, in particular, were shown to be considerably slower in terms of evaporation, water uptake, and viscosity and pour point changes. In OILMAP and SIMAP, in ice coverage between MIZ_{min} and MIZ_{max} (the pack ice threshold), i.e., in the MIZ, a linear reduction in wind speed influence on processes from the open-water value to zero in pack ice is applied to simulate shielding from wind effects. This reduces the evaporation, volatilization, emulsification, and entrainment rates due to reduced wind and wave energy.

In the oil in ice experiments by Brandvik et al. (2010a, 2010b), the evaporative loss of oils showed a significant difference between different ice conditions. The results indicate the difference in evaporative loss is mainly caused by the difference in oil film thickness, reflective of reduced spreading rate with oil slick thickening under higher ice coverage. Thus, this reduction in evaporative loss is reflected in model results via the reduced rate of spreading and constraints on surface area imposed by the ice cover.

SINTEF Sea Lab experiments (FEX2009, Brandvik et al. 2010b) showed that the presence of high ice coverage (90%) considerably slowed the rate and extent of the emulsification process as indicated from the percentage water uptake, presumably due to the significant wave damping and hence a reduction in wave mixing energy available for creating emulsions. In OILMAP and SIMAP, the maximum water content of emulsified oil decreases linearly from the open water unweathered oil value at MIZ_{min} to zero at 100% ice cover.

The extent of ice coverage also affects the rates of change of viscosity and oil density as a result of evaporative loss of light fractions and the uptake of water in the course of the water-in-oil emulsification process. Presence of ice slows and constrains oil spreading, and so slows the rate of evaporative weathering and the resulting oil viscosity and density increase as the oil weathers. Ice cover also reduces the emulsification rate, further slowing the rate of viscosity increase with weathering. The overall rate and extent of the viscosity increase was observed to be less in the dense ice coverage conditions of the FEX2009 field experiment (Brandvik et al. 2010b). The rates of change of physical-chemical and rhetorical properties of oil (e.g., viscosity) are also slowed as a result of weathering at low temperature, typical in conditions of partial ice coverage. Algorithms used for these processes are described in French McCay et al. (2017).

At a given oil viscosity, the droplet size distribution of entrained oil varies by ice cover, because of reduced entrainment rates in ice. Entrained oil droplets are larger under the lower energy conditions in the MIZ compared to open water wave conditions, and so in SIMAP dissolution from the droplets is reduced by lower surface area and reduced residence time in the water column (French-McCay et al. 2014). Dissolution of soluble aromatics proceeds for subsurface oil and oil under ice using the normal open-water algorithm (French-McCay 2004; French-McCay et al. 2017); however, the containment of oil in/under ice prolongs the exposure of surrounding water to the oil, resulting in higher dissolved concentrations in the local water parcel.

Degradation of subsurface and ice-bound oil occurs during all ice conditions, at rates occurring at the location (i.e., floating versus subsurface) without ice present. The rates are model inputs; biodegradation rates developed by French-McCay et al. (2015, 2016, 2017) based on literature review are typically used.

Simulations and Comparison to Field Drifter Data

Drifter buoys are deployed and tracked in the Arctic Ocean as part of the IABP to provide met-ocean data in real time. The IABP has deployed more than 700 buoys since it began operation in 1978. The number of buoys and the coverage varies each year, but an average of 25 buoys are in service at any time (Colony and Munoz 1986; Rigor and Ortmeyer 2001). The data are processed by the University of Washington's Polar Science Center, and are interpolated to produce gridded fields of surface temperature and velocity from drifter positions in 12-hour time steps (0000 UTM and 1200 UTM) daily. The interpolated position, and interpolated ice velocity fields, which are estimated and computed from the buoy positions, are available online from 1979 to present (Rigor 2002).

Drifter trajectories for buoys in the Beaufort Sea during years and areas where NERSC ice modeling products were available were extracted from IABP records. Oil spill model trajectories, using the NERSC (Ólason et al. 2016) data as input, were compared with the observed drifter trajectories. Simulations for locations in pack ice during winter-spring months were used to test the advancements of the neXtSIM model's EB ice rheology over the recently updated EVP rheology in the TOPAZ-EVP developed in Phase 1 and the publically-available TOPAZ4 model. TOPAZ-EVP-WIM includes the updated EVP rheology and a MIZ rheology that incorporates results of a Simulating WAves Nearshore (SWAN)-based wave model (Ólason et al. 2016), the performance of which was compared to the other models. With WIM included, the rheology in the MIZ was updated from the EVP version, so ice transport is expected to be different in this model. Since TOPAZ-EVP-WIM model results were available for March, June, September and December of 2008 and May of 2009, the comparisons were performed for all IABP observed trajectories available during those five months in the Beaufort Sea area covered by the NERSC products. As the neXtSIM model products were only provided for March, December and May, i.e., months where ice coverage was >90%, we focused the analysis on these "winter " months.

There were 61 drifters that moved through the TOPAZ-EVP-WIM study domain in the Beaufort Sea where we have data from all four ice model data products. IABP buoys were not available for the Kara-Barents Sea domain where NERSC data were provided.

The differences in the model-predicted versus observed tracks over time were measured to evaluate the model predictive skill. First, the trajectories of ice model and drifter data were plotted as progressive vector diagrams from the location of each drifter buoy at the selected initialization time, i.e., the first time step of the IABP trajectory section examined. The predicted and observed ice drifter trajectory were compared using a simple ratio of the model predicted path length divided by the observed path length. A dimensionless skill score was also calculated by using the Lagrangian separation distance between endpoints of simulated and observed drifters divided by the observed path length (Liu and Weisburg 2011; Ivichev et al. 2012). The separation index S is defined as:

$$S = \left(\sum_{i=1}^{N} sepDistance_i \Big/ \sum_{i=1}^{N} ObservedPath_i \right)$$

where $sepDistance_i$ is the separation distance and $ObservedPath_i$ is the cumulative length of the observed trajectory at time step i. N is the number of (e.g., 12-hour) time steps (segments of the trajectory) since the beginning of the simulation. Thus, the separation index S is a measure of the cumulative error in predicted distance traveled, normalized by the cumulative length of the observed trajectory. While S varies with the number of time steps, the time step is held constant at 12 hours matching the observational data. This approach accounts for the differences in the speeds of movement over the trajectory path. Differences in speed were evaluated using the ratio of the modeled to the observed path length (*LenRatio*).

The skill score *SS* is defined as: $SS = 1 - \left(\frac{S}{T}\right)$ for $S \leq T$ and $SS = 0$ for $S > T$.

T is a user-selected tolerance threshold that is typically set to 1. At $T = 1$, the tolerance for error is equal to the normalized cumulative separation distance, i.e., error should not exceed the magnitude of the cumulative movement. The skill score *SS* increases as model skill increases, but is zero if the model has "no skill", where *S* is greater than the tolerance threshold *T*.

An uncertainty estimate, in the form of a horizontal dispersion coefficient (*D*), may be computed for each simulation at time *t* since initialization as

$$D = \frac{sepDistance^2}{4t}$$

These estimates provide a potential value for the horizontal dispersion coefficient for oil spill modeling, accounting for uncertainty in the hydrodynamic & ice model.

Multiple drifter experiments were extracted from the IABP data set, trajectories simulated, and skill scores determined. The skill scores were then summarized and inter-compared. Drifter experiments were taken from continuous observed drifter trajectories, using the observed paths of individual buoys over 5-day, 10-day and 15-day non-overlapping intervals (i.e., sequences of segments of the IABP buoy paths that were 5, 10 or 15 days in length) that were within the ice model data domain and the temporal periods noted above. Five days is an appropriate and desirable forecast period for ice-ocean and oil spill modeling; the 10-day and 15-day intervals were examined to determine model skill farther into the future. The use of non-overlapping time periods ensures that the results are unbiased by auto correlations in the trajectory movements.

In addition to tabulating and examining the ratio of model to observed path lengths (relative speeds), and the *S* and *SS* skill scores, two-tailed student t-tests for unpaired observations were used to determine the significance of the differences. The subset of drifter intervals common to all four models, i.e., those in the smaller TOPAZ-EVP-WIM domain in the Beaufort Sea during March and December of 2008 and during 1-15 May of 2009, were examined in detail and compared using two-tailed student t-tests for paired observations.

May 2009 Field Experiment

The 2009 JIP experimental spill in the Barents Sea (FEX2009) east of Svalbard is the only available oil spill field experiment in the Arctic Ocean. Thus, it is desirable to verify the oil spill model with data on oil transport and fate from this experiment. The experiment took place northeast of Hopen Island and was planned to be under conditions of 50-70% ice in the MIZ (Brandvik et al. 2010b). However, at the time of the experiment, ice cover was 70-90%.

SIMAP was used to simulate the spill, utilizing the environmental data collected during the field experiment. The ice cover at the time of the experiment was 70-90% and so pack ice. The oil was observed to move with the ice. In the model, the movement of oil is with the ice under these conditions, so transport is dictated by the ice model used. The floe-contained oil drifted with the ice field ~80 km during the 6 day experimental period, according to Faksness et al. (2011). The neXtSIM model output was not available for the May 2009 period when the SINTEF field experiment was performed (i.e., the oil was released May 15, 2009; whereas the neXtSIM data provided ended on that date). The TOPAZ-EVP-WIM data set for the Barents and Kara Seas does cover all of May 2009, and it contains ice, current, and wind data, so it was used for the simulations.

The focus of the analysis was on evaluating the weathering in the model as compared to field measurements. The hindcast simulation results were compared to observations of the oil trajectory and fate and to the measured characteristics and movement of the ice field. Model predictions for the pack ice conditions were compared to observed oil weathering data.

The experimental conditions are summarized as:

- Location: 77.928^{o}N, 30.960^{o}E
- Data collection May 15-21, 2009
- Ice cover 70-90%
- Seawater temperature -1.8^{o}C
- Seawater salinity 34.3 psu
- Air temperature -2^{o}C to -10^{o}C
- Winds generally 5-10 m/s, peaking at 15-20 m/s during May 17-18
- Ice drift up to 100 cm/s during periods of strong winds

Fresh Troll B crude oil was released via a hose at a single point location and time on two dates (below). However, sampling was performed primarily on the main 7 m^3 release, so that spill is simulated by SIMAP.

- 7000 liters = 7 m^3 released May 15, 2009 over 30 minutes beginning at 0825 hrs (assumed CEST, so at 0625 UTC)
- 2000 liters = 2 m^3 released May 19, 2009 over 10 minutes at about 2200 hrs

At the location of the FEX2009 7 m^3 experiment, both the EB-based neXtSIM model and the TOPAZ-EVP-WIM model predicted 0% ice cover on May 15th, but the ice edge was nearby to the northeast. Thus, a nearby spill site (78.5^{o}N, 32.71^{o}E; 72 km northeast of the location of the experimental release) was selected as a proxy in an area where the TOPAZ-EVP-WIM model predicted 85-99% ice cover in the week following May 15, 2009. Other nearby sites were examined, but most were either >95% ice covered or open water with low ice cover. The 7 m^3 release of Troll B crude was modeled at both the actual site and the proxy pack-ice site.

The TOPAZ model quantified diffusion coefficients in the range of <0.1 - 4.9 m^2s^{-1} (Ólason et al. 2016). Results of NERSC's Discrete Element modeling indicated a diffusion coefficient of about 1 m^2s^{-1} in the MIZ. The diffusion coefficient would be lower in the pack ice. Thus, 1 m^2s^{-1} and 0.1 m^2s^{-1} were used in the oil spill modeling for the MIZ and pack ice, respectively.

Example Model Simulation in MIZ

The TOPAZ-EVP-WIM model accounted for the effects of sea ice on the wave field and ice break up by waves. In the TOPAZ-EVP-WIM model, where the maximum ice floe size was less than 250 m, NERSC changed the rheology from EVP to one appropriate to the MIZ (Ólason et al. 2016), so that would affect transport of both ice and oil within the ice in the MIZ.

The changes in characteristic wave heights, as well as weathering rates, spreading, oil thickness and oil properties, imposed by the presence and characteristics of sea ice, affect oil entrainment, transport and fate, as well as response operational windows such as *in situ* burning and dispersant use that increasingly lose effectiveness as the oil weathers. Thus, to evaluate differences in weathering induced by the wave model, the wave data from the TOPAZ-EVP-WIM model was used in place of the default wave model in SIMAP (and OILMAP). An arbitrary example spill site, in the general vicinity of the FEX2009 experimental site, was selected in an area where the TOPAZ-EVP-WIM model predicted 30-80% ice cover (characteristic of the MIZ) in the week following May 15, 2009. The SIMAP model was run using the same input assumptions as for the FEX2009 experimental site; the release location was simply moved (to the west, to 77.3°N, 24.0°E). As noted above, results of NERSC's Discrete Element modeling (Ólason et al. 2016) indicated a diffusion coefficient of about 1 m^2s^{-1} in the MIZ. Thus, 1 m^2s^{-1} was used in the oil spill modeling in the MIZ. The MIZ spill simulation using the TOPAZ-EVP-WIM wave data was compared to one at the same MIZ site using the default wave model in SIMAP, as well as to the simulations at the FEX2009 and proxy pack ice sites.

RESULTS

Comparisons of Model Predicted and Observed Drifter Trajectories

Trajectories of 61 drifters that moved through the TOPAZ-EVP-WIM study domain in areas of pack ice in the Beaufort Sea, where data from all ice model data products are available, were inspected visually. Examples are provided in the Supplementary Material (Figures S3-S5). In general, predicted trajectory patterns were similar (i.e., the trajectories overlaid each other overlapped), reflecting the underlying current and wind field inherent in all models. Performance was reasonably good for both TOPAZ-EVP and neXtSIM based simulations, as the model trajectories followed paths similar to the drifters. The transport paths are characterized by periods of relatively constant directional movement, interrupted by rapid changes in direction. There are typically three to five such events (i.e., storms or frontal passages) during the one month simulation period, although occasionally there are periods where motion is slow and buoys move in seemingly random directions. One can see divergences accumulate over time, but most of the displacements occur at the events.

Overall, the trajectory comparisons indicated the limits of the ice-ocean models' abilities to forecast as being about 7-15 days, although in some cases accuracy degrades considerably after 3-5 days of forecasting. This reflects the reliability of weather (i.e., wind) forecasts as being on this time scale and demonstrates the importance of accurate wind forecasts as input to ice models. While the accuracy of individual oil model trajectories projected weeks to months into the future would be expected to be low, in the event of a spill, forecasts could be updated frequently (on a time scale of hours to days) with satellite information, aircraft observations, drifter data, and other observations to improve reliability.

Accuracy of Ice-Ocean Model and Oil Spill Trajectory Forecasts

Forming conclusions based on visual inspection of trajectory maps is difficult and subjective, as many drifter trajectories need to be evaluated. Thus, to assess model skill and to avoid considering error accumulated over time, the skill scores of these and other drifter trajectories were calculated for short time intervals and examined. All the drifter intervals evaluated were in the pack ice, i.e., with ice coverage > 80%. The EB rheology is applicable in pack ice, so these comparisons test improvements afforded by use of the EB ice model against the various versions of ice models in TOPAZ using EVP rheology.

The ratios of model:observed path length (*LenRatio*), separation index (*S*) and skill scores (*SS*) calculated for each of the 5-day, 10-day and 15-day simulations of IABP drifter intervals using the different ice-ocean models are summarized for the winter months in Tables 3-5, respectively. The *LenRatio* and *S* are lowest using neXtSIM, highest using TOPAZ4 and intermediate using TOPAZ-EVP and TOPAZ-EVP-WIM as trajectory model inputs. The skill scores *SS* show the opposite pattern. The average skill scores are generally below 0.7. In intervals where the model skill is such that $S<1$, SS is calculated as >0, i.e., the model has some skill. The differences between skill scores for neXtSIM, TOPAZ-EVP and TOPAZ4 are significant at $p<0.05$ for the 5-day and 10-day trajectories, and are significant at $p<0.10$ for the 15-day trajectories, based on a two-tailed *t*-test for unpaired observations (SD = standard deviation). The differences between the *LenRatio* and *S* indices between the models were of slightly less significance (because of higher variance than *SS*, which treats all poor fitting model trajectories equally as no skill). TOPAZ-EVP-WIM simulations were intermediate in performance between TOPAZ-EVP and neXtSIM, but the differences compared to these two models were not significant. Thus, the SS results indicate that the neXtSIM model has better skill than both TOPAZ models with standard EVP rheology, but results for neXtSIM do not show significantly better performance than TOPAZ-EVP-WIM simulations with NERSC's updated EVP rheology (Ólason et al. 2016) in the MIZ.

Note that TOPAZ-EVP-WIM are hourly data, whereas data for TOPAZ-EVP and neXtSIM were provided as 6-hour averages, and TOPAZ4 data provided on the web are daily averaged vectors. However, model skill in the winter months was not lowered by the time-averaging. Model trajectories in March, December and May within pack ice using the TOPAZ-EVP-WIM ice vectors averaged over 6 hours and over 24 hours did not produce significantly different results from the trajectories using hourly data.

The *LenRatio* results for the winter months (Tables 3-5) indicate that the model-predicted ice drift speeds are faster than observed, more so for the TOPAZ models than for neXtSIM. However, examination of results by month showed that the speeds were too high (speeds averaged 5-8 times the observed for the 5-day trajectories, Table S1) for all models in March

2008, but neXtSIM, TOPAZ-EVP and TOPAZ-EVP-WIM were not significantly different from the observed in December 2008 and May 2009, whereas TOPAZ4 speeds averaged 1.5 times the observed (Table S2). Model skill (SS) was much lower for March 2008 than for December 2008 and May 2009 (Tables S1-S2). In December 2008 and May 2009, model performance was relatively good for simulations 10 days and 15 days in length (Tables S3 and S4), and while neXtSIM performed significantly better than TOPAZ4, TOPAZ-EVP-WIM performed as well as neXtSIM by all three metrics.

The *LenRatio*, *S* and *SS* scores for each of the 5-day, 10-day and 15-day drifter intervals using each ice-ocean model were calculated for the summer months (Tables S5-S7). The results are not significantly different using TOPAZ4, TOPAZ-EVP and TOPAZ-EVP-WIM as trajectory model inputs. However, using TOPAZ-EVP-WIM as hourly data, 6-hour means and 24-hour means yields different trajectories and calculated *S* and *SS* scores in June and September of 2008. The differences in *S* and *SS* are significant ($p<0.05$) after 10 days and 15 days of forecast, but after 5 days, only the trajectory using 24-hour time averaging is significantly different from the trajectory using the 1-hour data. The *LenRatio* results are not significantly different. The differences induced by the time averaging were in trajectory directions and not path length (speed) because averaging altered the patterns of the rapid changes in direction (see examples in Figures S3 and S4). In the pack ice in winter, time averaging did not change the trajectories, likely because of fewer and less dramatic rapid changes in direction.

The Separation distance (km) between the model trajectory and the observed path provides a simple metric of the difference in the forecasted position after 5-day, 10-day or 15-days of model simulation. Separation distances after 5 days (Table 6) are on average 20-22 km using the

TOPAZ models (based on results for all 5 months) and 14 km using neXtSIM (in the winter months). Table 6 shows that the expected separation distances increase to about 45 km for TOPAZ and 26 km for neXtSIM after 15 days. The coefficient of variation is 70-80% of the mean for TOPAZ and 62-64% of the mean for neXtSIM.

The hydrodynamic model in TOPAZ4 is a reanalysis version (i.e., it assimilated environmental data), whereas the hydrodynamic models in the TOPAZ-EVP and TOPAZ-EVP-WIM simulations were free run with no data assimilation. The current data in TOPAZ-EVP-WIM and TOPAZ4 Reanalysis were used for model simulations of IABP buoys in <30% ice (assumed open water in the oil trajectory model). There were 26 5-day drifter intervals in the September 2008 TOPAZ-EVP-WIM domain, allowing direct comparisons between the hydrodynamics models' performances. TOPAZ4 Reanalysis showed statistically better ($p<0.01$) skill than TOPAZ-EVP-WIM (Table 7). Given the similar performance of the ice models coupled to these two TOPAZ hydrodynamic models, the TOPAZ-EVP-WIM's updated EVP and MIZ rheology performed better than the standard EVP rheology in TOPAZ4.

In addition, the neXtSIM model was run with different currents and winds than the TOPAZ models. The neXtSIM model used a recent reanalysis version of TOPAZ hydrodynamics and ASR Final Reanalysis winds (i.e., both assimilated environmental and remote-sensing data), whereas TOPAZ-EVP and TOPAZ-EVP-WIM were free run with no data assimilation and used ERA Interim (ECMWF) winds. It is not clear how much these differences contributed to the different performance of the ice models against the IABP drifter observations.

Example Trajectories in Operational Mode

Figures S6 to S9 in the Supplementary Material demonstrate for a single example drifter (#66276), tracked in March and April 2008, the TOPAZ4, TOPAZ-EVP, TOPAZ-EVP-WIM and neXtSIM model-predicted trajectories compared to the observed trajectory, respectively. The model-predicted trajectories are reinitialized to the observed locations every 5 days. The simulations with re-initialization show improved matches to the observations. All of the models perform well in this operational mode where the modeled locations are updated regularly.

May 2009 Field Experiment

The field test confirmed that ice can act as a natural barrier, confine oil to reduce spreading, and slow the rate of weathering. The oil drifted with the ice, as it was contained between the ice floes (Faksness et al. 2010, 2011).

Winds were generally 5-10 m/s during the experimental period. Winds increased to 6 m/s the night of May 16, peaking at 15-20 m/s during May 17-18 (Faksness et al. 2010; Figures S10-S11). ERA Interim winds at the experimental and proxy sites ("Pack Ice") were similar to the measured winds (Figure S11). The measured currents at 5 m depth averaged 16.7 cm/s and varied from 0.2 cm/s to 50.7 cm/s (Faksness et al. 2010). The modeled currents by TOPAZ-EVP-WIM were in the same range as the measured currents for the first 2.5 days (through May 17) but modeled currents were slower than observed later during the experiment (Figure S12).

The modeled ice speeds by TOPAZ-EVP-WIM at the experimental site and the proxy site in the pack ice were very different (Figure S13). In the TOPAZ-EVP-WIM model, there was <30% ice cover at the experimental site May 18-20, whereas the ice cover was in reality 70-90%. During the 6 day experiment, the ice field was observed to drift nearly 80 km (Brandvik et al.

2010b). Ice drifted up to 100 cm/s during periods of strong winds on May 17-18 (Figure S14). The shift in weather conditions from initially calm and moderate to strong wind speed with a sudden change of wind direction at day three of the experiment resulted in enhanced spreading of the oil slick (Faksness et al. 2011).

The oil was observed to move with the ice to 10 km N and then to 40 km S of the spill site (50 km total range of trajectory North/South, Figure S14). The oil reached 30 km to the east of the spill site (30 km total range of trajectory East/West). The ice drift averaged about 3% of wind speed and was angled about 20-50 degrees to the right of downwind (Faksness et al. 2010). The initial slick was 30 m x 20 m at 0900 hrs on the 15th of May, just after release. On the 16th, 17th, 18th and 20th of May the slick was stretched to 100 m, 300 m, 1000 m, and 3000 m, respectively (Brandvik et al. 2010b; Faksness et al. 2010).

The model trajectory from the experimental site (Figure S15) moved 176 km to a position 124 km south of the release location. This is much faster than observed, however, note the TOPAZ-EVP-WIM model does not predict ice cover in the area where the experiment occurred. The model trajectory from the proxy site in pack ice moved 56 km to a position 44 km south of the release location (Figures S16 and S17). Between May 19 and 20th, the north-south stretched slick moved to the east. Thus, the trajectory in the pack ice was similar to the observed.

Figures 1 and 2 show the estimated lengths and areas of the oil slick over time in the model trajectories, as compared to observations reported in Brandvik et al. (2010b) and Faksness et al. (2010). After day 2 the model trajectory in the pack ice area is more elongated than observed, likely due to entrainment into slower currents under the ice than occurred in the field, since this elongation pattern is created by the difference between the wind-driven surface oil movements and the subsurface entrained oil that resurfaces behind the leading edge of the oil.

Figures 3 and 4 show the modeled mass balance of the oil in the simulations. Note that in the model for the experimental site most of the oil remains on the surface and evaporates in time, whereas the model in the pack ice area shows dramatic entrainment into the water column during the gale on May 17-18, followed by resurfacing of the oil after the storm. This entrainment was facilitated by the low degree of weathering of the oil by that time in the pack ice, where spreading was much slower than in the open water situation in the simulation at the experimental site. The entrainment in the pack ice simulation resulted in a greatly elongated slick as the entrained oil resurfaced behind the slick. This phenomenon was observed, but the observed slick was not as long as the results for the model at the proxy site in the pack ice.

The field-collected data included oil viscosity, water content of emulsions, density of water free oil, oil evaporative loss, oil pour point, UV fluorometry data (as a tracer for total petroleum hydrocarbons) and measured concentrations of semi-soluble hydrocarbons (e.g., naphthalenes, 2-3 ring PAHs, 4-6 ring PAHs, and decalins) in the water column (Faksness et al. 2010; Brandvik et al. 2010b). The UV fluorometry data measured 3 m below the slick did not sense presence of concentrations of oil or soluble components in the water column (Brandvik et al. 2010b). However, detectable concentrations of dissolved hydrocarbons (primarily alkylated phenols, naphthalenes and 3-ring PAHs) were measured at concentrations of 0.1 – 1.5 ppb in the water column under the oil slick before May 20th when additional oil was released and burned. Estimated concentrations of dissolved hydrocarbons based on semi-permeable membrane devices (SPMDs) were 0.6 – 4 ppb (Faksness et al. 2010). The model predicted concentrations of dissolved hydrocarbons were 0.1 – 2.3 ppb in the experimental site simulation and 0.1 – 2.4 ppb in the pack ice simulation.

The water content of the oil and the oil viscosity were observed to increase to 44% water in the emulsion and to a viscosity varying between ~200 and 2200 cp on May 18-19 (Brandvik et al. 2010b). The model predicted maximum water contents were 75% in the experimental site simulation and 50% in the pack ice simulation. The model predicted viscosities were ~20,000 cp in the experimental site simulation and varied between 400 cp and 1400 cp on May 18-19 in the pack ice simulation. The observed evaporative loss was about 30% by the end of the experiment; the model simulations predicted about 28% loss by the end of May 17th and 40% evaporative loss by May 20.

Thus, overall the model simulation in the pack ice predicted similar results to the experimental observations. However, the different location appears to have somewhat different currents and potentially other environmental conditions. The sudden divergence of the model in pack ice from the observed beginning on May 18th at two days after oil release (Figures 3-4) suggests conditions were not the same after this time. Comparison of the results of the two model simulations clearly shows the dramatic effect of ice cover on weathering and transport of the oil.

Example Model Simulation in MIZ

The ERA Interim winds at the MIZ location to the west of the FEX2009 site were similar to the winds at the experimental and proxy sites (“Pack Ice”), but speeds were lower during the storm period on days 2 and 3 after the release (Figure S11). The modeled currents and ice movements by TOPAZ-EVP-WIM were different at the MIZ site than at the experimental and proxy pack ice sites (Figures S12 and S13). The model trajectory in the MIZ shows more eastward movement than the simulations at the FEX2009 and proxy sites (Figure S18).

Figures 5 and 6 show the modeled mass balance of the oil in the simulations at the MIZ site. The use of the wave data from the TOPAZ-EVP-WIM model in place of the default (USACE, 2002) wave model in SIMAP had only a small effect on the mass balance. The MIZ simulations show dramatic entrainment during the storm May 17-18, similar to the simulation in the pack ice, while in the simulation at the experimental site most of the oil remained on the surface (compare Figure 6 to Figures 3 and 4). Oil spreading was reduced and oil weathering (e.g., evaporation and emulsification) rates were slowed in both the MIZ and the pack ice simulations, as compared to the open water simulation at the experimental site. Reduced oil weathering rates within ice, both in the field experiment and in the model, slowed the rate of increase in oil viscosity, and, as a result, entrainment was higher during periods of high winds.

DISCUSSION AND CONCLUSIONS

Use of Ice-Ocean Model Data Products

OILMAP and SIMAP may use inputs from any coupled ice-ocean model that outputs netCDF (network Common Data Format) data, a convention utilized by oil spill and other particle transport models. Thus, new coupled ice-ocean models applicable to specific Arctic regions can be brought online quickly and easily, giving responders the ability to rapidly take advantage of new modeling technologies and products as they evolve.

Protocols for provision of hydrodynamics and ice data and their attributes (i.e., the metadata) in the netCDF format are now standard. For use in trajectory modeling, both current and ice data should be provided together, on the same grid and coordinate system and at the same time steps. The meteorological data (i.e., winds) used for forcing should also be provided or identified (from operational models available on line). In addition, based on the results of this study, for good predictive forecast modeling, the time steps of the hydrodynamics and ice model results used as input should be much more frequent than daily (such as 3 hrs), and not time averaged. The present TOPAZ4 model is provided on the web as daily means.

Regardless of these operational and logistic issues, the ice-ocean model needs to resolve the region of interest in sufficient detail for oil spill modeling to be of operational assistance. In other regions outside the Arctic, meso-scale and locally-focused models provide more detail. In the future, nesting of meso-scale models in areas of interest would provide more detail than possible with an ocean-scale model.

Accuracy of Ice-Ocean Model and Oil Spill Trajectory Forecasts

Rampal et al. (2016b) compared modeled trajectories using their updated ice model products with IABP drifter paths, examining speeds and diffusivities, finding the EB-based neXtSIM model more closely agreed with the IABP observations than TOPAZ-EVP. They found that in general, trajectories were longer when modeled using the TOPAZ data than observed in the IABP data. They noted that short IABP trajectories towards the Canadian Arctic Archipelago (seen in 2007/2008 winter) corresponded to the piling up of thick ridged sea ice, and that this dynamical sea ice response is captured by the EB-based neXtSIM model but not by the EVP model in the TOPAZ system. Examining the results for the three months with pack ice where EB applies and where we were able to compare model trajectories to drifters (March 2008, December 2008 and May 2009), we can confirm these findings for 5-day trajectories in

December 2008 and May 2009 where predicted speeds using TOPAZ4 were ~1.4 times the observed, while the EB-based predicted speeds agreed well with the observed (Table S2). However, the March 2008 5-day drifter simulations we performed (Table S1) showed that TOPAZ-EVP overestimated drifter speeds by a factor 5.2 - 8.3 on average, and the EB-based neXtSIM model path lengths were on average 4.7 times the observed. Many of the March-2008 drifters appeared to become trapped in landfast ice, which may account for the poor performance of all the models that month.

Nevertheless, overall our findings based on the modeled trajectories herein (Tables 3-5, S1-S4), as measured by the ratio of modeled to observed path lengths (indicative of relative speed) and skill scores, are consistent with Rampal et al.'s (2016b) findings related to relative performance. A comprehensive test series involving statistical comparisons of the modeled trajectories to ~400 5, 10, 15 and 30-day intervals of IABP drifter trajectories demonstrated that the new neXtSIM model predictions agree more closely with the observations than the operational status quo models represented by TOPAZ4 using the older (standard) EVP rheology. There was a significant improvement in the forecast performance (as measured by cumulative divergence from the observed buoy path) in TOPAZ accomplished with the Phase I TOPAZ-EVP model, and the neXtSIM EB model trajectories were significantly better than both the Phase I TOPAZ-EVP and TOPAZ4 models in speed and direction of oil-in-ice movements. On average, over all months tested, the neXtSIM EB model trajectories were statistically similar in length to the observed buoys (i.e., indicating similar speed of ice movements), whereas oil trajectories using the TOPAZ models using standard EVP rheology had significantly longer lengths 1.5 up to 5 times longer than the paths of the observational buoys.

Based on the present analysis, use of the neXtSIM model with EB rheology would improve the accuracy of oil spill trajectory and fate modeling in areas of pack ice when compared to the use of results from TOPAZ with EVP rheology. At present, the TOPAZ4 model is run operationally, as well as in hindcast reanalysis mode, and its daily averages are freely available on a public website. National and private agencies commonly use TOPAZ4 for operational forecasts of sea ice drift, as well as for hindcasts, spill planning and risk analyses. Availability of neXtSIM ice-ocean model results in netCDF-compliant format could improve forecasting and these other analyses in areas of extensive pack ice.

From the sample of drifters examined here, it appears that the updated TOPAZ-EVP and TOPAZ-EVP-WIM models perform better than the publically-available TOPAZ4 reanalysis version, but this may be due in part to differences in the wind forcing used (while all three models used interim ERA winds, TOPAZ4 may have been run with an earlier version) and/or to the daily averaging used to deliver (on the web) the TOPAZ4 product as compared to 6-hourly or hourly data delivered in the TOPAZ-EVP and TOPAZ-EVP-WIM products, respectively.

While time averaging does not appear to make a significant difference for short (5-day) intervals, for longer forecasts the averaging erases sudden changes in direction seen in buoy trajectories and introduces error. Provision of TOPAZ-EVP model data at smaller time steps (than daily, as on the web server, or even than 6-hourly) and without time averaging would provide for improved performance in oil spill modeling. When the oil spill model utilized the same high-resolution ice vector data as used by NERSC in Phase 1 (Ólason et al. 2016) for simulating drifter trajectories (Figure S19), the results agreed, whereas the use of time-averaged data degraded the model performance and the drift tracks diverged somewhat from the actual buoy tracks recorded.

Further analysis would provide more insight as to the locations, times and conditions under which these noted improvements in model performance should be expected. In using these ice model products for oil spill forecast modeling, one needs to consider the increasing divergence between model predicted and observed trajectories of drifters in ice that accumulate over time using any of the ice model products. Separation distances after 5 days are on average 20-22 km using the TOPAZ models and 14 km using neXtSIM (in the winter months). The statistics presented in this study (Tables S1 – S7) provide uncertainty estimates that could be used in forecasting. The accuracy of individual oil model trajectories projected more than a few days into the future would be expected to be low, recognizing that beyond this time scale the wind forecast accuracy degrades quickly, as would the hydrodynamic and ice model forecasts dependent upon wind forcing. In practice, operational oil spill trajectory forecasts should be frequently re-initialized to reduce the forecast errors that are accumulated from the initial locations (Liu and Weisberg, 2011; Ivichev et al. 2012). All of the models examined here perform well with frequent reinitialization.

In any case, the overall transport patterns and results of an ensemble of trajectories would provide useful information for planning and risk assessments based on typical current and ice movement patterns. For such applications, use of reanalysis winds, currents and ice data, or continuously updated operational model results (i.e., a time series of reinitialized forecasts run for short intervals with observational data assimilation), would characterize the range of potential trajectories. Based on the findings here, in pack ice the speed of oil movements using neXtSIM would be expected to be more accurate than those using TOPAZ4 with the operational EVP rheology. Similar analysis of model performance in the MIZ would be useful to characterize uncertainties in areas of lower ice cover.

Ice Drift Speeds and Dispersion

Comparisons made by NERSC (Ólason et al. 2016) of the ice models with the IABP data quantified uncertainty in the form of a horizontal dispersion coefficient that is a function of separation distance varying with forecast time. NERSC described how this information can be used in oil spill models to forecast likely positions over time. If an oil spill model is run with this horizontal dispersion coefficient, the cloud of Lagrangian Elements representing the oil will encompass the uncertainty envelope, accounting for uncertainty in the hydrodynamic & ice model.

For the period of 2007 to 2010, Ólason et al. (2016) calculated the mean drift and ice dispersion rates of the IABP buoys, and compared these to the TOPAZ-EVP and neXtSIM (EB) model estimates (Table 8). NERSC concluded that the TOPAZ model does not represent correctly the mean and the fluctuating part of the ice motion. The mean and fluctuating motion are overestimated by about 30-40% and the absolute diffusivity by about 100%. The EB model performs better at representing the absolute diffusivity. It underestimated the mean and fluctuating motion by about 10-20% and provides the same value of absolute diffusivity as observations.

May 2009 Field Experiment

SIMAP was used to simulate the FEX2009 7 m^3 experimental spill, utilizing the environmental data collected during the field experiment. The ice cover at the time of the experiment was 70-90% and so pack ice. The oil was observed to move with the ice. In the model, the movement of oil is with the ice under these conditions, so transport is dictated by the ice model used. The neXtSIM model output was not available for the May 2009 period when the SINTEF field experiment was performed (i.e., the oil was released May 15, 2009; whereas the neXtSIM data provided ended on that date). The TOPAZ-EVP-WIM data set for the Barents and Kara Seas does cover all of May 2009, and it contains ice, current, and wind data, so it was used for the simulations.

At the location of the FEX2009 7 m^3 experiment, both the EB-based neXtSIM model and the TOPAZ-EVP-WIM model predicted 0% ice cover on May 15th. Thus, a nearby spill site (78.5°N, 32.71°E) was selected as a proxy in an area where the TOPAZ-EVP-WIM model predicted 85-99% ice cover in the week following May 15, 2009.

Overall the model simulation at the proxy site in the pack ice predicted similar results to the experimental observations. Comparison of the results of the two model simulations clearly showed the dramatic effect of ice cover on weathering and transport of the oil. In the model in pack ice, weathering was greatly slowed by the ice cover, in agreement with observations in the field and in the laboratory (Brandvik et al. 2010a,b).

Example Model Simulation in MIZ

The model results show that oil spreading is reduced and oil weathering (e.g., evaporation and emulsification) rates are slowed in both MIZ and heavy ice conditions, as compared to in open water. Reduced oil weathering rates within ice slows the rate of increase in oil viscosity, and, as a result, entrainment rates of oil into the water column are higher during periods of high winds. These model results are in agreement with the observations made in the field (May 2009 experiment) and in the laboratory (Brandvik et al. 2010a,b), as described above.

Conclusions

A comprehensive test series involving statistical comparisons of the modeled trajectories to ~400 intervals of 5, 10, 15 and 30-days from IABP drifter trajectories demonstrated that the new neXtSIM model predictions agree more closely with the observations than the operational status quo models represented by TOPAZ4 using the older (standard) EVP rheology, in agreement with findings by Rampal et al. (2016b). However, all of the models performed well in operational mode where the modeled locations are updated regularly (every 5 days) with locations of field-deployed drifters.

While time averaging does not appear to make a significant difference for short (5-day) intervals, for longer forecasts the averaging erases sudden changes in direction (due to storms and frontal passages) seen in buoy trajectories and introduces error. Provision of ice-ocean model data at smaller time steps (than daily, as presently publically-available, or even than 6-hourly) and without time averaging would provide for improved performance to oil spill modeling.

SIMAP was used to simulate the FEX2009 7 m^3 experimental spill, utilizing the environmental data collected during the field experiment. The ice cover at the time of the experiment was 70-90% (i.e., pack ice). Overall the model simulation in the pack ice predicted similar results to the experimental observations. Comparison of the results of model simulations in open water and in pack ice clearly showed the dramatic effect of ice cover on weathering and transport of the oil. In the model in pack ice, weathering was greatly slowed by the ice cover, in agreement with observations in the field and in the laboratory.

ACKNOWLEDGEMENTS

This research is part of the International Association of Oil and Gas Producers (IOGP), Arctic Oil Spill Response Technology – Joint Industry Programme (JIP) supported by nine oil and gas companies – BP, Chevron, ConocoPhillips, Eni, ExxonMobil, North Caspian Operating Company, Shell, Statoil, and Total.

REFERENCES

Afenyo, M., Veitch, B. and Khan, F. 2016. A state-of-the-art review of fate and transport of oil spills in open and ice-covered water. Ocean Eng. 119: 233-248.

ASCE Task Committee on Modeling Oil Spills. 1996. State-of-the-art Review of Modeling Transport and Fate of Oil Spills. Water Resources Engineering Division, ASCE, J. Hydraul. Eng. 122(11): 594-609.

Bear, J. and Verruijt, A. 1987. Modeling Groundwater Flow and Pollution with Computer Programs for Sample Cases. Kluwer Academic Publishers.

Bleck, R. 2002. An oceanic general circulation model framed in hybrid isopycnic-cartesian coordinates. Ocean Modell. 4: 55-88.

Brandvik, P.J. and Faksness, L.-G. 2009. Weathering processes in Arctic oil spills: Meso-scale experiments with different ice conditions. Cold Reg. Sci. Technol.. 55(1): 160-166.

Brandvik, P.J. Daling, P.S. and Myrhaug, J.L. 2010a. Mapping weathering properties as a function of ice conditions: a combined approach using a flume basin verified by large scale field experiments. *In* Proceedings of the 33rd Arctic and Marine Oilspill Program Technical Seminar. Environment Canada. Ottawa, ON. Canada. 33: 701-723.

Brandvik, P.J., Daling, P.S., Faksness, L.-G., Fritt-Rasmussen, J., Daae, R.L., and Leirvik, F. 2010b. Experimental oil release in broken ice – a large-scale field verification of results from laboratory studies of oil weathering and ignitability of weathered oil spills. SINTEF Materials and Chemistry, Oil in Ice – JIP Report No. 26, 38p. http://www.sintef.no/project/JIP_Oil_In_Ice/dokumenter/publications/ JIP-rep-no-26-FEX2009-weathering-ISB-final.pdf.

Coastal Response Research Center (CRRC). 2016. State-of-Science for Dispersant Use in Arctic Waters: Physical Transport and Chemical Behavior. Coastal Response Research Center, University of New Hampshire, Durham, NH. February 29, 2016, 18p.

Colony, R. and Munoz, E.A. 1986. Arctic Ocean Buoy Program, Data Report 1Jan.1984-31 Dec.1985. Published Oct.1986: ftp://iabp.apl.washington.edu/pub/IABP/C/; http://nsidc.org/data/G00791; http://nsidc.org/data/docs/noaa/g00791_iabp/index.html.

Drozdowski, A., Nudds, S., Hannah, C.G., Niu, H., Peterson, I., and Perrie, W. 2011. Review of Oil Spill Trajectory Modelling in the Presence of Ice. Canadian Technical Report of Hydrographic and Ocean Sciences. 274: vi + 84p.

Evensen, G. 1994. Sequential data assimilation with nonlinear quasi-geostrophic model using Monte Carlo methods to forecast error statistics. J. Geophys. Res. 99: 10143-10162.

Faksness L.-G., Daae, R.L., Brandvik, P.J., Leirvik, F., Børseth, J.F. 2010. Oil distribution and bioavailability: Field experiment FEX 2009. SINTEF Materials and Chemistry, Oil in Ice – JIP Report No. 33, 978-82-14-05012-7. SINTEF, Trondheim, Norway, September 20, 2010. https://www.sintef.no/globalassets/project/jip_oil_in_ice/dokumenter/publications/jip-rep-no-33-fex2009-oil-distribution-and-bioavailability.pdf.

Faksness, L.-G., Brandvik, P.J., Daae, R.L., Leirvik, F. and Børseth, J.F. 2011. Large-scale oil-in-ice experiment in the Barents Sea: Monitoring of oil in water and MetOcean interactions. Mar. Pollut. Bull. 62(5): 976-984.

French-McCay, D.P. 2002. Development and application of an Oil Toxicity and Exposure Model, OilToxEx. Environ. Toxicol. Chem. 21: 2080-2094.

French-McCay, D.P. 2003. Development and application of damage assessment modeling: example assessment for the North Cape oil spill. Mar. Pollut. Bull. 47(9-12): 341-359.

French-McCay, D.P. 2004. Oil spill impact modeling: development and validation. Environ. Toxicol. Chem. 23(10): 2441-2456.

French-McCay, D., Gearon, M.S., Kim, Y.H., Jayko, K. and Isaji, T. 2014. Modeling oil transport and fate in the Beaufort Sea. *In* Proceedings of the 37th Arctic and Marine Oilspill Program Technical Seminar. Environment Canada. Ottawa, ON. Canada. 37: 40-64.

French-McCay, D., Jayko, K., Li, Z., Horn, M., Kim, Y., Isaji, T., Crowley, D., Spaulding, M., Fontenault, J., Shmookler, R. and Rowe, J. 2015. Technical Reports for Deepwater Horizon Water Column Injury Assessment WC_TR.14: Modeling Oil Fate and Exposure Concentrations in the Deepwater Plume and Rising Oil Resulting from the Deepwater Horizon Oil Spill; Date of Report: September 29, 2015. Project No, 2011-144. RPS ASA, 55 Village Square Drive, South Kingstown, RI 02879. DWH-AR0285776. https://www.doi.gov/deepwaterhorizon/adminrecord

French-McCay, D.P, Li, Z., Horn, M., Crowley, D., Spaulding, M., Mendelsohn, D., and Turner, C. 2016. Modeling Oil Fate and Subsurface Exposure Concentrations from the Deepwater

Horizon Oil Spill. *In* Proceedings of the 39th AMOP Technical Seminar on Environmental Contamination and Response, Environment Canada. 39:115-150.

French-McCay, D.P., Jayko, K., Li, Z., Horn, M., Isaji, T., and Spaulding, M. 2017, in press. Simulation Modeling of Ocean Circulation and Oil Spills in the Gulf of Mexico – Appendix II Oil Transport and Fates Model Technical Manual. Prepared by RPS ASA for the US Department of the Interior, Bureau of Ocean Energy Management, Gulf of Mexico OCS Region, New Orleans, LA. OCS Study BOEM 20xx-xxx. xxx pp.

Haapala, J., Lönnroth, N. and Stössel, A. 2005. A numerical study of open water formation in sea ice. J. Geophys. Res. 110: C09011. doi:10.1029/2003JC002200.

Hunke, E.C. and Dukowicz, J.K. 1997. An Elastic-Viscous-Plastic model for sea ice dynamics. J. Phys. Oceanogr. 27: 1849-1867.

Ivichev, I., Hole L. R., Karlin, L., Wettre, C. and Röhrs, J. 2012. Comparison of operational oil spill trajectory forecasts with surface drifter trajectories in the Barents Sea. J. Geol. Geosci. 1: 105.

Lee, K., Boudreau, M., Bugden, J., Burridge, L., Cobanli, S.E., Courtenay, S., Grenon, S., Hollebone, B., Kepkay, P., Li, Z., Lyons, M., Niu, H, King, T.L., MacDonald, S., McIntyre, E.C., Robinson, B., Ryan, S.A. and Wohlgeschaffen ,G. 2011. State of Knowledge Review of Fate and Effect of Oil in the Arctic Marine Environment. Report prepared for National Energy Board of Canada, Centre for Offshore Oil, Gas and Energy Research (COOGER), Fisheries and Oceans Canada, Bedford Institute of Oceanography, Dartmouth, Nova Scotia, Canada, 267p.

Liu, Y. and Weisberg, R.H. 2011. Evaluation of trajectory modeling in different dynamic regions using normalized cumulative Lagrangian separation. J. Geophys. Res. 116: C09013.

Mårtensson, S., Meier, H. E. M., Pemberton, P. and Haapala, J. 2012. Ridged sea ice characteristics in the Arctic from a coupled multicategory sea ice model. J. Geophys. Res. 117: C00D15, doi:10.1029/2010JC006936.

Ólason, E., Bouillon, S. and Rampall, P. 2016. Sea ice model developments in view of oil spill forecasting. ART JIP Oil Spill Trajectory Modeling Programme. NERSC Technical Report, Bergen, Norway, 17 February 2016, 56p. http://www.arcticresponsetechnology.org/wp-content/uploads/2016/06/Trajectory-Modelling-Report-Final.pdf.

Peterson, I.K., Prinsenberg, S., and Holladay, J.S. 2008. Observations of sea ice thickness, surface roughness and ice motion in Amundsen Gulf. J. Geophys. Res. 113: C06016. doi:10.1029/2007JC004456.

Rampal, P. S. Bouillon, E. Ólason, and M. Morlighem. 2016a. neXtSIM: a new Lagrangian sea ice model. Cryosphere. 10: 1055-1073. doi:10.5194/tc-10-1055-2016.

Rampal, P., S. Bouillon, J. Bergh, and E. Ólason. 2016b. Arctic sea-ice diffusion from observed and simulated Lagrangian trajectories. Cryosphere. 10:1513–1527. doi:10.5194/tc-10-1513-2016.

Rigor, I. G. 2002. IABP Drifting Buoy Pressure, Temperature, Position, and Interpolated Ice Velocity, Version 1. [C data]. Compiled by Polar Science Center, Boulder, Colorado USA. NSIDC: National Snow and Ice Data Center, January 2016. http://dx.doi.org/10.7265/N53X84K7.

Rigor, I. and Ortmeyer, M. 2001. International Arctic Buoy Program Data Report 1 Jan.2000-31 Dec.2000. Applied Physics Laboratory, University of Washington, Seattle, Washington, 98105-6698, April 2001. http://iabp.apl.washington.edu/data.html.

Sakov, P., Counillon, F., Bertino, L., Lisæter, K. A., Oke, P. R., and Korablev, A. 2012. TOPAZ4: an ocean-sea ice data assimilation system for the North Atlantic and Arctic. Ocean Sci. 8: 633-656. doi:10.5194/os-8-633-2012.

Sørstrøm, S.E., Brandvik, P.J., Buist, I., Daling, P.S., Dickins, D., Faksnes, L.-G., Potter, S., Rasmussen, J.F. and Singaas, I. 2010. Joint industry program on oil spill contingency for Arctic and ice-covered waters. Oil in ice – JIP Summary report. Report no. 32. SINTEF Materials and Chemistry. October 04, 2010. http://www.sintef.no/globalassets/project/jip_oil_in_ice/dokumenter/publications/jip-rep-no-32-summary-report.pdf.

Spaulding, M.L. 1988. A State-of-the-Art Review of Oil Spill Trajectory and Fate Modeling. J. Oil Chem. Pollut. 4: 39-55.

US Army Corps of Engineers (USACE). 2002. Coastal Engineering Manual. Engineer Manual 1110-2-1100, U.S. Army Corps of Engineers, Washington, D.C. (in 6 volumes); Meteorology and Wave Climate. *In* Coastal Engineering Manual, Part II , Chapter II-2 , 1 August 2008 (Change 2). http://140.194.76.129/publications/eng-manuals/EM_1110-2-1100_vol/PartII/Part_II-Chap_2.pdf.

Venkatesh, S., El-Tahan, H., Comfort, G., and Abdelnour, R. 1990. Modelling the behaviour of oil spills in ice-infested waters. Atmos.-Ocean, Canadian Meteorological and Oceanographic Society. 28(3): 303-329.

Youssef, M. 1993. The behavior of the near ocean surface under the combined action of waves and currents in shallow water. PhD Dissertation, Department of Ocean Engineering, University of Rhode Island, Narragansett, RI.

Youssef, M. and Spaulding, M.L. 1993. Drift current under the action of wind waves. *In* Proceedings of the 16th Arctic and Marine Oil Spill Program Technical Seminar. Calgary, AB, Canada. 16: 587-615.

Youssef, M. and Spaulding, M.L. 1994. Drift Current Under the Combined Action of Wind and Waves in Shallow Water. *In* Proceedings of the 17th Arctic and Marine Oil Spill Program (AMOP) Technical Seminar. Vancouver, BC. 17: 767-784.

TABLE CAPTIONS

Table 1. NERSC data products and web sources for hydrodynamic and wind data used by NERSC (Ólason et al. 2016) for the ice-ocean modeling that generated these data products.

Table 2. Oil fate and behavior processes applied in OILMAP and SIMAP.

Table 3. Summary of the ratios of model:observed path length (LenRatio), separation index (S) and skill scores (SS) using each ice-ocean model for transport calculations compared to the observed drifter trajectories, using 5-day simulations for non-overlapping intervals in the winter-ice periods 1-25 March 2008, 1-30 December 2008 and 1-15 May 2009.

Table 4. Summary of the ratios of model:observed path length (LenRatio), separation index (S) and skill scores (SS) using each ice-ocean model for transport calculations compared to the observed drifter trajectories, using 10-day simulations for non-overlapping intervals in the winter-ice periods 1-25 March 2008, 1-30 December 2008 and 1-15 May 2009.

Table 5. Summary of the ratios of model:observed path length (LenRatio), separation index (S) and skill scores (SS) using each ice-ocean model for transport calculations compared to the observed drifter trajectories, using 15-day simulations for non-overlapping intervals in the winter-ice periods 1-25 March 2008, 1-30 December 2008 and 1-15 May 2009.

Table 6. Summary of the expected separation distances between model and observed drifters after 5, 10 and 15 days, using each ice-ocean model for transport calculations (all months: March, June, September, December 2008; May 2009).

Table 7. Skill scores (SS) for drifters in open water.

Table 8. Mean drift and ice dispersion rates of the IABP buoys, TOPAZ-EVP and neXtSIM (EB) model estimates (Ólason et al. 2016).

FIGURE CAPTIONS

Figure 1. Estimated length of the oil slick over time, in model trajectories and observed.

Figure 2. Estimated area of the oil slick over time, in model trajectories and observed.

Figure 3. Modeled mass balance for the trajectory released at the experimental site.

Figure 4. Modeled mass balance for the trajectory released at the proxy site in pack ice.

Figure 5. Modeled mass balance for the trajectory released at the MIZ site using the wave, currents and ice data from the TOPAZ-EVP-WIM model.

Figure 6. Modeled mass balance for the trajectory released at the MIZ site using the default wave model in SIMAP and currents and ice data from the TOPAZ-EVP-WIM model.

TABLES

Table 1. NERSC data products and web sources for hydrodynamic and wind data used by NERSC (Ólason et al. 2016) for the ice-ocean modeling that generated these data products.

Trajectory	Ice Model Used	Hydrodynamic Model Used to Run Ice Model	Winds Used	Time Steps and Periods[d]
IABP drifter	Observed drifter positions	(n.a.)	(n.a.)	12-hourly
neXtSIM EB Model (JIP Phase 1)	EB	TOPAZ-Reanalysis[a]	ASR Final Reanalysis[b]	6-hourly time-averaged data; 10 winter periods (i.e., November 1 – May 15, for 2000-2010)
TOPAZ-EVP (JIP Phase 1)	EVP	TOPAZ free run (Phase 1)	ERA Interim (ECMWF)[c]	6-hourly time-averaged data; 10 years (2001-2010)
TOPAZ-EVP-WIM (JIP Phase 1)	EVP & MIZ	TOPAZ free run (Phase 1)	ERA Interim (ECMWF)[c]	1-hourly time-averaged data during 5 individual months (March, June, September, and December of 2008 and May 2009)
TOPAZ4-Operational Reanalysis (Public)	EVP	TOPAZ4-Operational Reanalysis[a]	ERA Interim (ECMWF)[c]	Daily means; 7 years

[a] TOPAZ reanalysis [http://marine.copernicus.eu/web/69-interactive-catalogue.php?option=com_csw&view=details&product_id=ARCTIC_REANALYSIS_PHYS_002_003]
[b] ASR Final 30 km 2D surface forecast [http://rda.ucar.edu/datasets/ds631.0/]
[c] ERA Interim (ECMWF) [http://www.ecmwf.int/en/research/climate-reanalysis/era-interim]
[d] The horizontal resolution of the TOPAZ and neXtSIM models was approximately 12-16 km in the Arctic Ocean.

Table 2. Oil fate and behavior processes applied in OILMAP and SIMAP.

Description	**Ice Cover (Percent)**	**Advection**	**Evaporation & Emulsification**	**Entrainment and Volatilization**	**Spreading**
Open Water and Drift Ice	$\leq MIZ_{min}$	Surface oil moves as in open water	As in open water	As in open water	As in open water
MIZ: Ice Patches and Leads	MIZ_{min} – MIZ_{max}	Surface oil moves with the ice	Linear reduction in wind speed with ice cover to 0% at MIZ_{max}	Linear reduction in wind speed with ice cover to 0% at MIZ_{max}	Constrained by open water area
Pack Ice (Heavy Ice) and Landfast Ice	$\geq MIZ_{max}$	Surface oil moves with the ice (or remains still in landfast ice)	None (evaporation if on top of ice)	None	None

Table 3. Summary of the ratios of model:observed path length (*LenRatio*), separation index (*S*) and skill scores (*SS*) using each ice-ocean model for transport calculations compared to the observed drifter trajectories, using 5-day simulations for non-overlapping intervals in the winter-ice periods 1-25 March 2008, 1-30 December 2008 and 1-15 May 2009.

Ice-Ocean Model	**Drifters (#)**	**Intervals (#)**	***LenRatio* Mean**	***LenRatio* SD**	***S* Mean**	***S* SD**	***SS* Mean**	***SS* SD**
TOPAZ4 Reanalysis, 24-hr mean	34	132	4.41	8.33	3.02	7.10	0.35	0.29
TOPAZ-EVP, 6-hr mean	34	132	3.51	6.48	2.30	5.35	0.41	0.30
TOPAZ-EVP-WIM, 1 hr mean	34	132	2.81	4.96	1.81	3.82	0.46	0.30
neXtSIM EB model, 6-hr mean	34	132	2.56	5.19	1.65	4.38	0.49	0.30

Table 4. Summary of the ratios of model:observed path length (*LenRatio*), separation index (*S*) and skill scores (*SS*) using each ice-ocean model for transport calculations compared to the observed drifter trajectories, using 10-day simulations for non-overlapping intervals in the winter-ice periods 1-25 March 2008, 1-30 December 2008 and 1-15 May 2009.

Ice-Ocean Model	Drifters	Intervals	*LenRatio*	*LenRatio*	*S*	*S*	*SS*	*SS*
	(#)	(#)	Mean	SD	Mean	SD	Mean	SD
TOPAZ4 Reanalysis, 24-hr mean	34	59	2.57	5.10	1.20	3.52	0.43	0.31
TOPAZ-EVP, 6-hr mean	34	59	2.06	3.32	0.80	1.75	0.50	0.29
TOPAZ-EVP-WIM, 1 hr mean	34	59	1.52	1.36	0.54	0.47	0.54	0.27
neXtSIM EB model, 6-hr mean	34	59	1.39	1.81	0.45	0.49	0.60	0.21

Table 5. Summary of the ratios of model:observed path length (*LenRatio*), separation index (*S*) and skill scores (*SS*) using each ice-ocean model for transport calculations compared to the observed drifter trajectories, using 15-day simulations for non-overlapping intervals in the winter-ice periods 1-25 March 2008, 1-30 December 2008 and 1-15 May 2009.

Ice-Ocean Model	**Drifters (#)**	**Intervals (#)**	***LenRatio* Mean**	***LenRatio* SD**	***S* Mean**	***S* SD**	***SS* Mean**	***SS* SD**
TOPAZ4 Reanalysis, 24-hr mean	32	39	1.54	0.51	0.50	0.40	0.54	0.24
TOPAZ-EVP, 6-hr mean	32	39	1.26	0.45	0.41	0.29	0.61	0.22
TOPAZ-EVP-WIM, 1 hr mean	32	39	1.08	0.34	0.37	0.21	0.63	0.19
neXtSIM EB model, 6-hr mean	32	39	0.94	0.29	0.31	0.16	0.69	0.16

Table 6. Summary of the expected separation distances between model and observed drifters after 5, 10 and 15 days, using each ice-ocean model for transport calculations (all months: March, June, September, December 2008; May 2009).

Model	Days	Mean Separation distance (km)	Coefficient of Variation
TOPAZ4 Reanalysis	5	21	0.73
	10	34	0.72
	15	44	0.75
TOPAZ-EVP	5	22	0.77
	10	37	0.76
	15	45	0.73
TOPAZ-EVP-WIM	5	20	0.73
	10	34	0.69
	15	45	0.73
neXtSIM EB model	5	14	0.64
	10	21	0.64
	15	26	0.62

Table 7. Skill scores (SS) for drifters in open water.

Statistic	Fraction Ice Cover	TOPAZ-EVP-WIM	TOPAZ4 Reanalysis
Mean	5.63×10^{-4}	0.346	0.469
Standard Deviation	2.87×10^{-3}	0.230	0.247
#	26	26	26

Table 8. Mean drift and ice dispersion rates of the IABP buoys, TOPAZ-EVP and neXtSIM (EB) model estimates (Ólason et al. 2016).

IABP or Model	Mean Drift Speed (cm/s)	Fluctuating Component of Ice Drift (cm/s)	Absolute Diffusivity (cm^2/s)
IABP	2.45	6.90	8
TOPAZ-EVP	3.38	8.97	15
neXtSIM	2.00	6.14	8

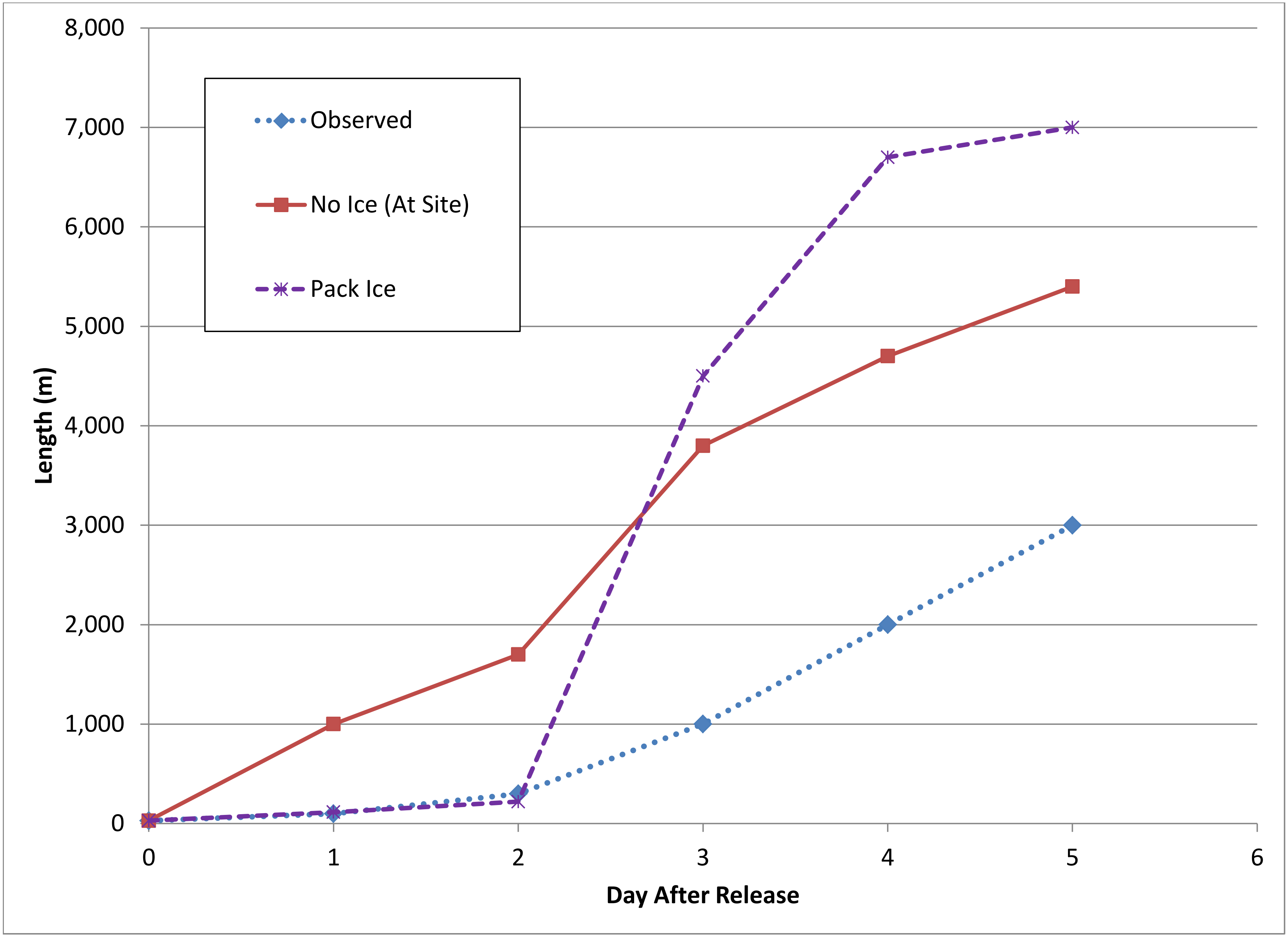
Observed
No Ice (At Site)
Pack Ice
8,000
7,000
6,000
5,000
4,000
3,000
2,000
1,000
0
Length (m)
0
1
2
3
4
5
6
Day After Release

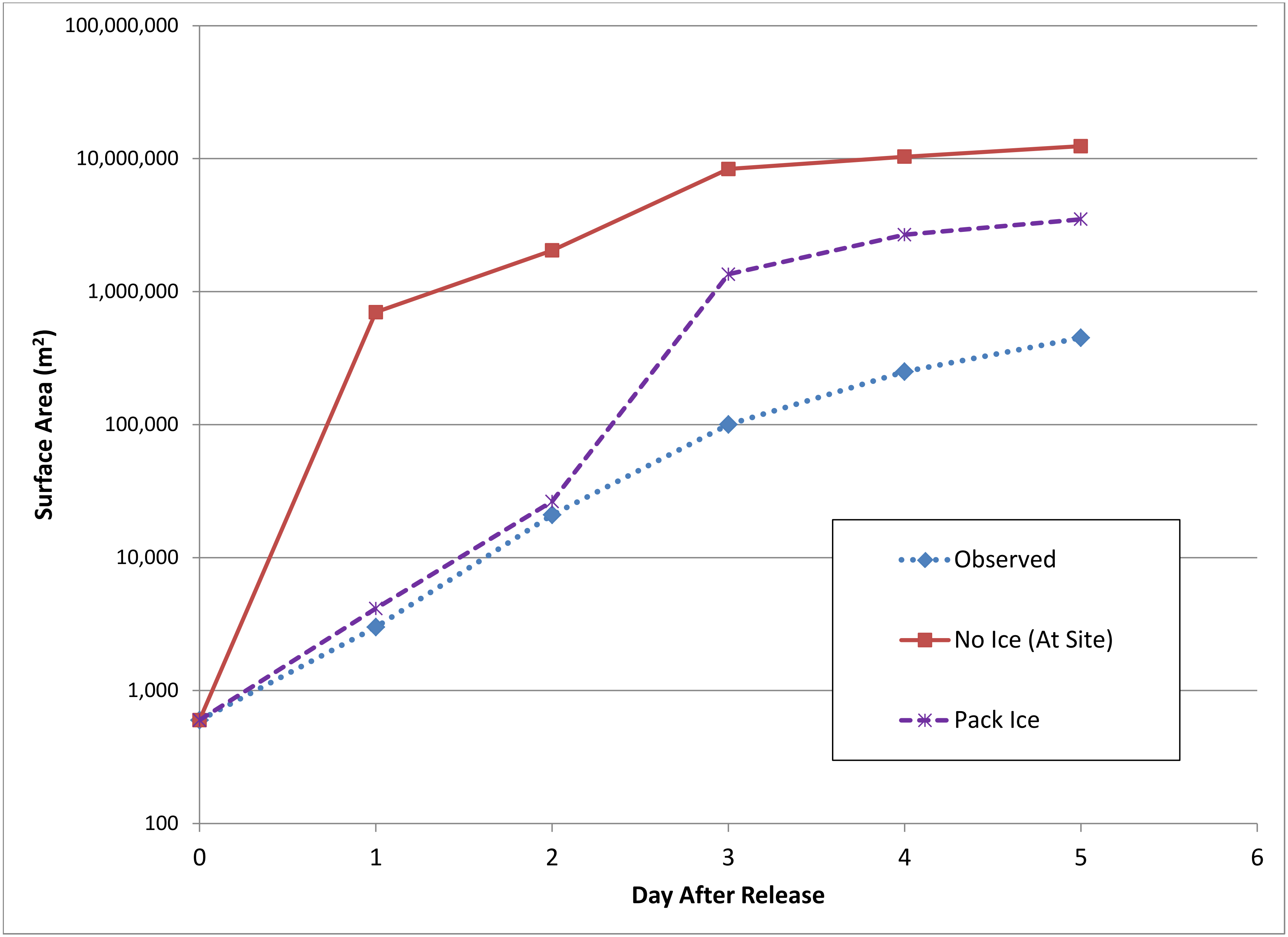
100,000,000
10,000,000
1,000,000
100,000
10,000
1,000
100
Surface Area (m²)
0
1
2
3
4
5
6
Day After Release
Observed
No Ice (At Site)
Pack Ice

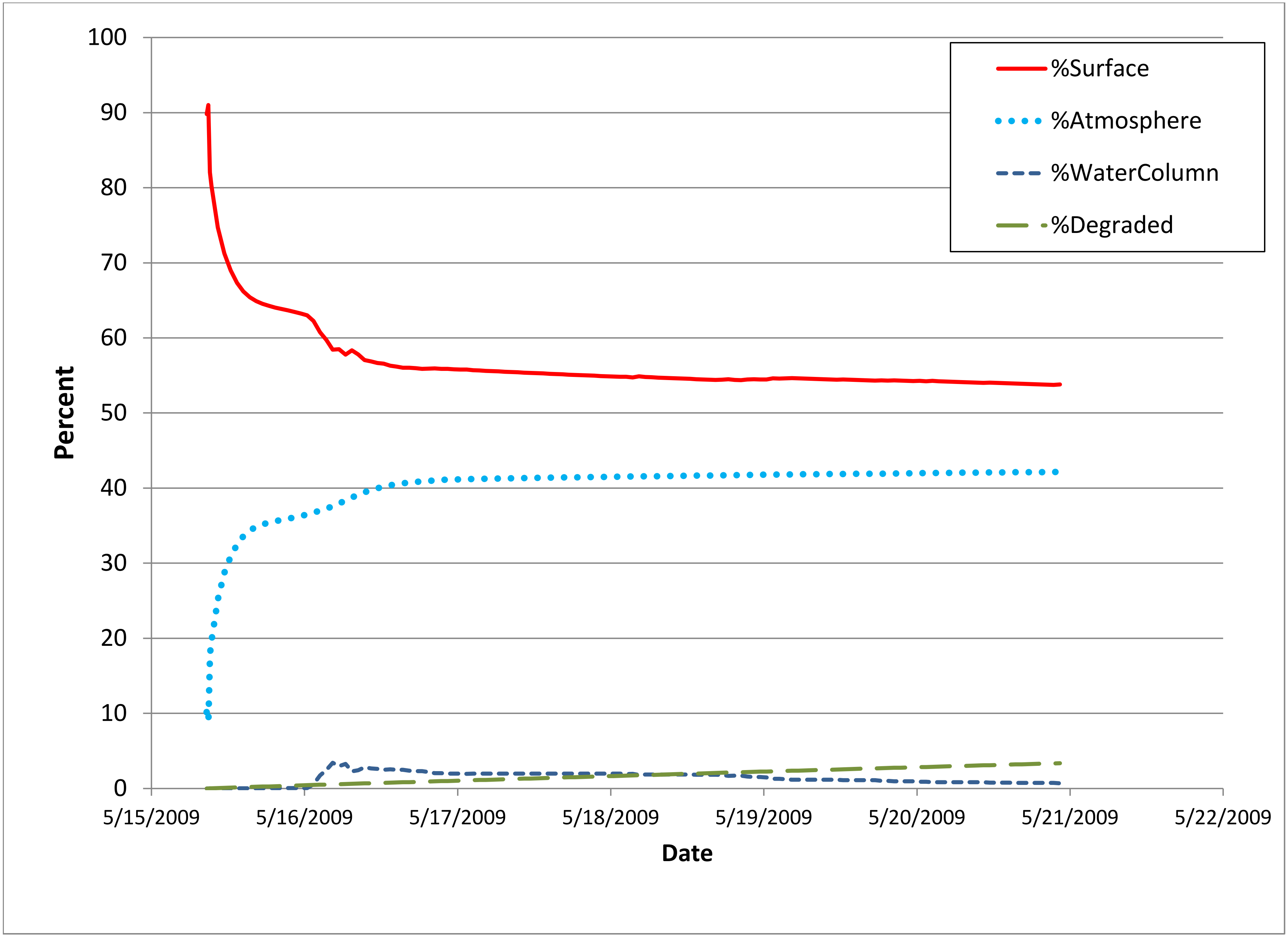
100
90
80
70
60
50
40
30
20
10
0
Percent
5/15/2009
5/16/2009
5/17/2009
5/18/2009
5/19/2009
5/20/2009
5/21/2009
5/22/2009
Date
%Surface
%Atmosphere
%WaterColumn
%Degraded

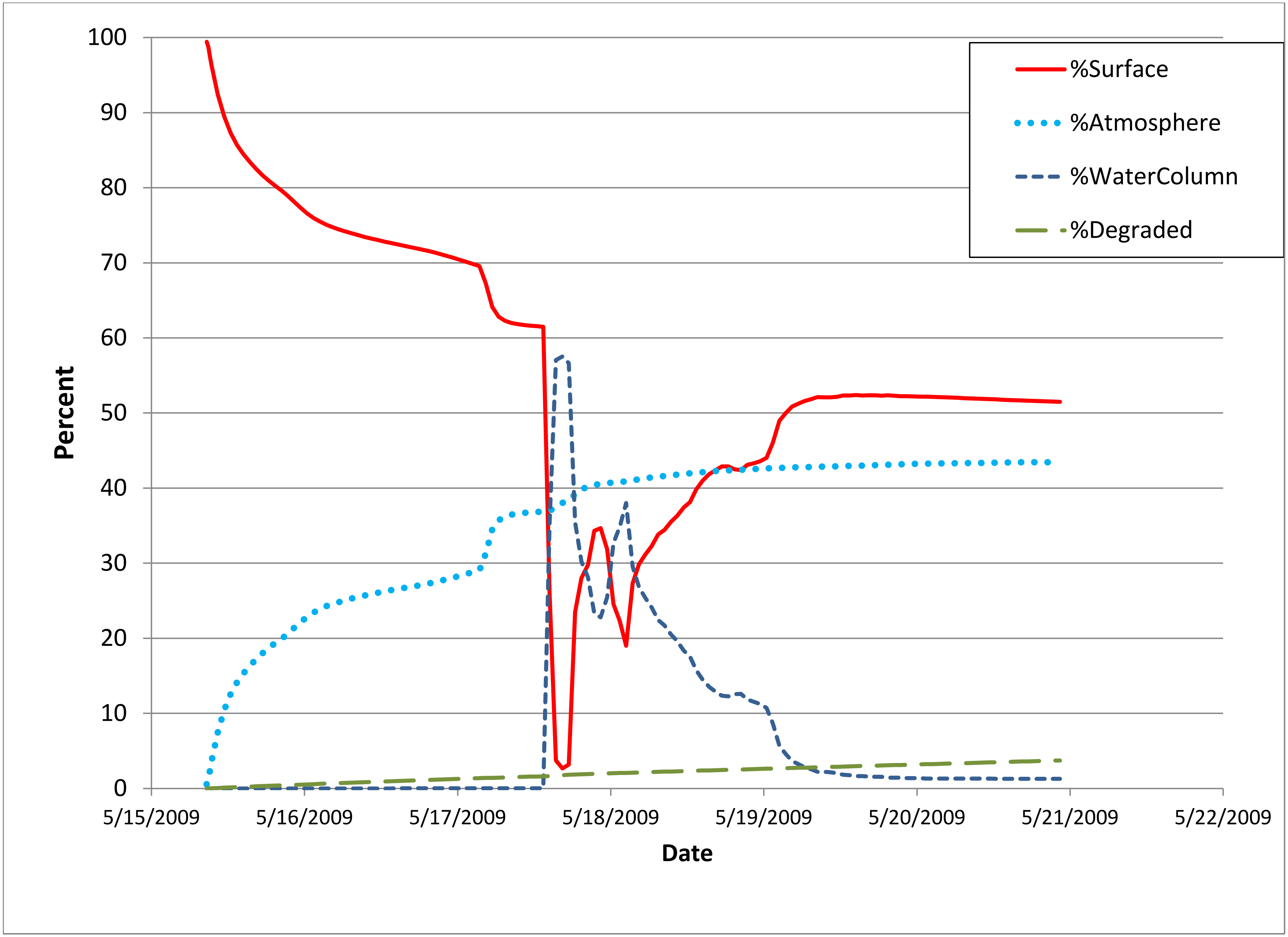
100
90
80
70
60
50
40
30
20
10
0
Percent
5/15/2009
5/16/2009
5/17/2009
5/18/2009
5/19/2009
5/20/2009
5/21/2009
5/22/2009
Date
%Surface
%Atmosphere
%WaterColumn
%Degraded

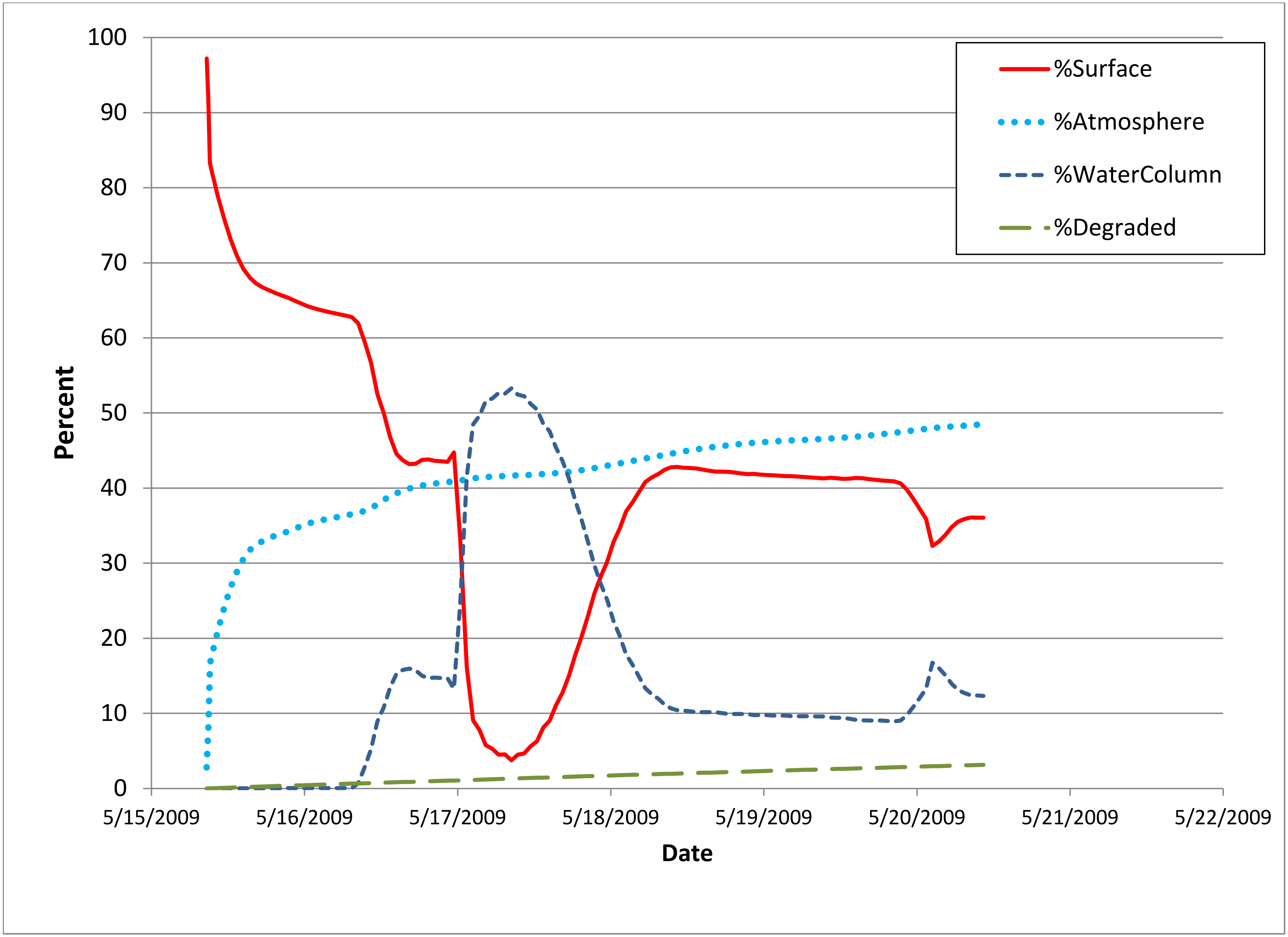
100
90
80
70
60
50
40
30
20
10
0
Percent
5/15/2009
5/16/2009
5/17/2009
5/18/2009
5/19/2009
5/20/2009
5/21/2009
5/22/2009
Date
%Surface
%Atmosphere
%WaterColumn
%Degraded

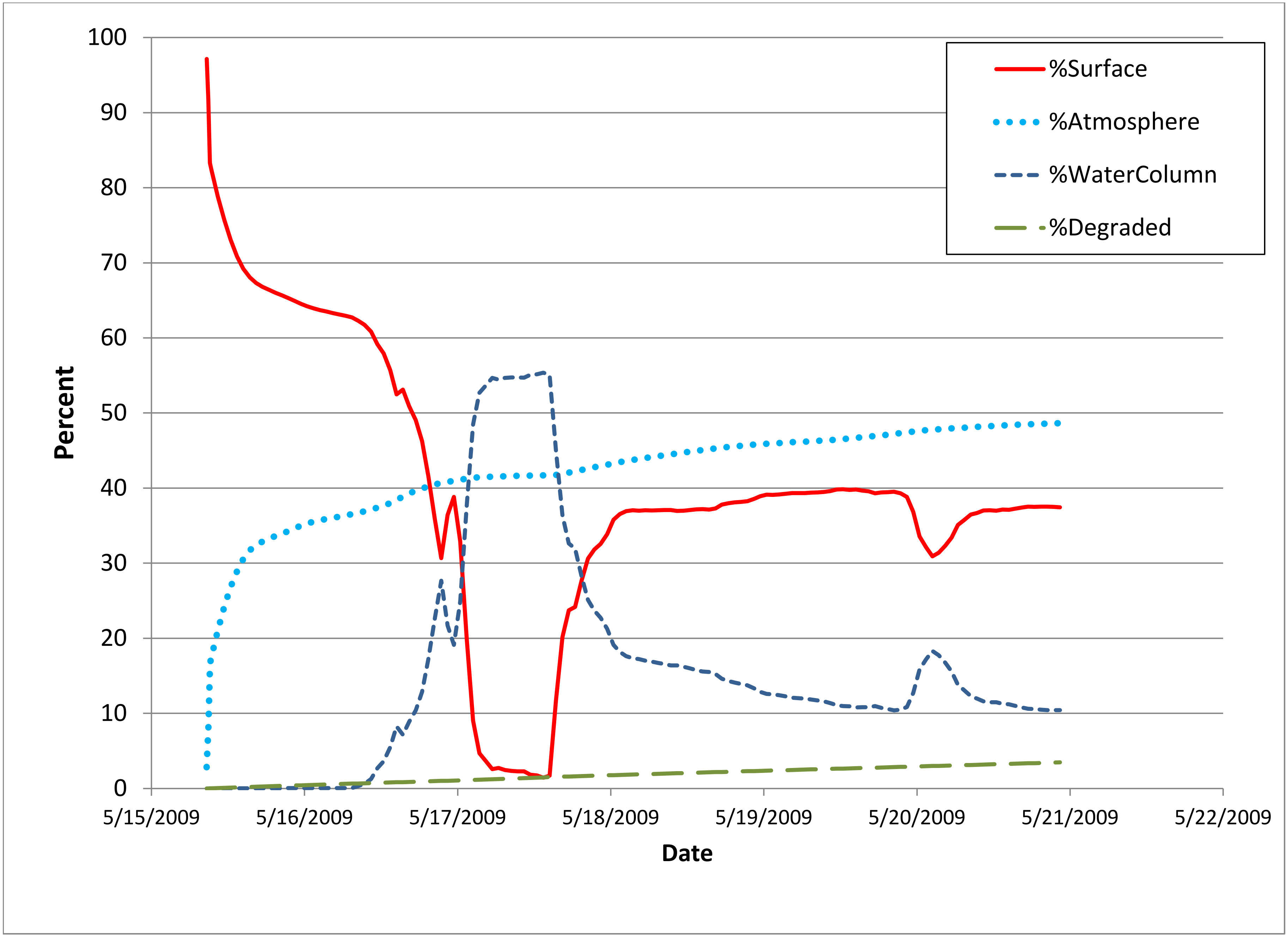

100
90
80
70
60
50
40
30
20
10
0
Percent
5/15/2009
5/16/2009
5/17/2009
5/18/2009
5/19/2009
5/20/2009
5/21/2009
5/22/2009
Date
%Surface
%Atmosphere
%WaterColumn
%Degraded